



# Network Analysis Reveals Different Cellulose Degradation Strategies Across *Trichoderma harzianum* Strains Associated With XYR1 and CRE1

Rafaela Rossi Rosolen<sup>1,2</sup>, Alexandre Hild Aono<sup>1,2</sup>, Déborah Aires Almeida<sup>1,2</sup>,  
Jaíre Alves Ferreira Filho<sup>1,2</sup>, Maria Augusta Crivelente Horta<sup>1</sup> and Anete Pereira De Souza<sup>1,3\*</sup>

<sup>1</sup>Center for Molecular Biology and Genetic Engineering (CBMEG), University of Campinas (UNICAMP), Campinas, Brazil,

<sup>2</sup>Graduate Program in Genetics and Molecular Biology, Institute of Biology, University of Campinas (UNICAMP), Campinas, Brazil,

<sup>3</sup>Department of Plant Biology, Institute of Biology, University of Campinas (UNICAMP), Campinas, Brazil

## OPEN ACCESS

### Edited by:

Ka-Chun Wong,  
City University of Hong Kong, Hong  
Kong SAR, China

### Reviewed by:

Vivek Sharma,  
Chandigarh University, India  
Bishwo Adhikari,  
Plant Protection and Quarantine,  
Animal and Plant Health Inspection  
Service (USDA), United States

### \*Correspondence:

Anete Pereira De Souza  
anete@unicamp.br

### Specialty section:

This article was submitted to  
Computational Genomics,  
a section of the journal  
Frontiers in Genetics

**Received:** 01 November 2021

**Accepted:** 04 February 2022

**Published:** 24 February 2022

### Citation:

Rosolen RR, Aono AH, Almeida DA,  
Ferreira Filho JA, Horta MAC and  
De Souza AP (2022) Network Analysis  
Reveals Different Cellulose  
Degradation Strategies Across  
*Trichoderma harzianum* Strains  
Associated With XYR1 and CRE1.  
*Front. Genet.* 13:807243.  
doi: 10.3389/fgene.2022.807243

*Trichoderma harzianum*, whose gene expression is tightly controlled by the transcription factors (TFs) XYR1 and CRE1, is a potential candidate for hydrolytic enzyme production. Here, we performed a network analysis of *T. harzianum* IOC-3844 and *T. harzianum* CBMAI-0179 to explore how the regulation of these TFs varies between these strains. In addition, we explored the evolutionary relationships of XYR1 and CRE1 protein sequences among *Trichoderma* spp. The results of the *T. harzianum* strains were compared with those of *Trichoderma atroviride* CBMAI-0020, a mycoparasitic species. Although transcripts encoding carbohydrate-active enzymes (CAZymes), TFs, transporters, and proteins with unknown functions were coexpressed with *cre1* or *xyr1*, other proteins indirectly related to cellulose degradation were identified. The enriched GO terms describing the transcripts of these groups differed across all strains, and several metabolic pathways with high similarity between both regulators but strain-specific differences were identified. In addition, the CRE1 and XYR1 subnetworks presented different topology profiles in each strain, likely indicating differences in the influences of these regulators according to the fungi. The hubs of the *cre1* and *xyr1* groups included transcripts not yet characterized or described as being related to cellulose degradation. The first-neighbor analyses confirmed the results of the profile of the coexpressed transcripts in *cre1* and *xyr1*. The analyses of the shortest paths revealed that CAZymes upregulated under cellulose degradation conditions are most closely related to both regulators, and new targets between such signaling pathways were discovered.

**Abbreviations:** ABC, ATP-binding cassette; CAZymes, carbohydrate-active enzymes; CCR, carbon catabolite repression; CEs, carbohydrate esterases; CNT, concentrative nucleoside transporter; CRE1, carbon catabolite repressor 1; GHs, glycoside hydrolases; GO, Gene Ontology; GTs, glycosyltransferases; HRR, highest reciprocal rank; iTOL, Interactive Tree of Life; ITS, internal transcribed spacer; JTT, Jones-Taylor-Thornton; K2P, Kimura two-parameter; KEGG, Kyoto Encyclopedia of Genes and Genomes; KO, KEGG Orthology; MEGA, Molecular Evolutionary Genetics Analysis; MFS, major facilitator superfamily; ML, Maximum likelihood; PLs, polysaccharide lyases; Ta0020, *Trichoderma atroviride* CBMAI-0020; *tefl1*, translational elongation factor 1; TFs, transcription factors; Th0179, *Trichoderma harzianum* CBMAI-0179; Th3844, *Trichoderma harzianum* IOC-3844; TOM, topological overlap matrix; TPM, transcripts per million; WGCNA, weighted correlation network analysis; XYR1, xylanase regulator 1.

Although the evaluated *T. harzianum* strains are phylogenetically close and their amino acid sequences related to XYR1 and CRE1 are very similar, the set of transcripts related to *xyr1* and *cre1* differed, suggesting that each *T. harzianum* strain used a specific regulation strategy for cellulose degradation. More interestingly, our findings may suggest that XYR1 and CRE1 indirectly regulate genes encoding proteins related to cellulose degradation in the evaluated *T. harzianum* strains. An improved understanding of the basic biology of fungi during the cellulose degradation process can contribute to the use of their enzymes in several biotechnological applications and pave the way for further studies on the differences across strains of the same species.

**Keywords:** *Trichoderma harzianum*, *Trichoderma atroviride*, cellulose, transcription factors, coexpression networks

## 1 INTRODUCTION

Lignocellulosic biomass is a complex recalcitrant structure that requires a consortium of carbohydrate-active enzymes (CAZymes) for its complete depolymerization. Due to their unique ability to secrete these proteins efficiently, filamentous fungi, such as *Trichoderma* spp. and *Aspergillus* spp., are widely explored for the industrial production of CAZymes (de Assis et al., 2015; Bischof et al., 2016). In the genus *Trichoderma*, *Trichoderma reesei* is the primary fungal industrial source of cellulases and hemicellulases (Martinez et al., 2008), while *Trichoderma harzianum* and *Trichoderma atroviride* have been widely explored by examining their biocontrol capacity against plant pathogenic fungi (Medeiros et al., 2017; Saravanakumar et al., 2017). However, hydrolytic enzymes from *T. harzianum* strains have demonstrated great potential in the conversion of lignocellulosic biomass into fermentable sugars (Delabona et al., 2020; Zhang et al., 2020).

The production of CAZymes in filamentous fungi is controlled at the transcriptional level by several positive and negative transcription factors (TFs) (Benocci et al., 2017). In *T. reesei*, the Zn<sub>2</sub>Cys<sub>6</sub>-type TF xylanase regulator 1 (XYR1) is described as the most important activator of cellulase and xylanase gene expression (Stricker et al., 2006). During growth on an induction carbon source, XYR1 was shown to be synthesized *de novo* and degraded at the end of induction (Lichius et al., 2014). Although XYR1 orthologs are present in almost all filamentous ascomycete fungi, the molecular mechanisms triggered by this regulator depend on the species (Klaubauf et al., 2014). In *T. atroviride*, the induction of genes that encode cell wall-degrading enzymes considered relevant for mycoparasitism, such as *axe1* and *swo1*, is influenced by XYR1 (Reithner et al., 2014). In *T. harzianum*, the overexpression of *xyr1* increases the levels of the reducing sugars released in a shorter time during saccharification (Delabona et al., 2017). Overall, in the genus *Trichoderma*, XYR1 evolved by vertical gene transfer (Druzhinina et al., 2018).

In the presence of easily metabolizable carbon sources, such as glucose, the expression of *xyr1* and genes encoding lignocellulose-degrading enzymes is repressed by carbon catabolite repression (CCR), which is regulated by the C<sub>2</sub>H<sub>2</sub>-type TF carbon catabolite repressor 1 (CRE1) (Strauss et al., 1995; Mach-Aigner et al., 2008; Alazi and Ram 2018). Upon glucose depletion, the concentration

of CRE1 in the nucleus rapidly decreases, and CRE1 is recycled into the cytoplasm (Lichius et al., 2014). Furthermore, the phosphorylation of CRE1 plays an essential role in signal transduction to achieve CCR (Horta et al., 2019; Han et al., 2020). CRE1 is the only conserved TF throughout the fungal kingdom, suggesting a conserved mechanism for CCR in fungi (Adnan et al., 2017). Interestingly, the effect of *cre1* deletion on the gene expression profile of its targets varies among species. In *T. reesei* RUT-C30, the deletion of a full *cre1* can lead to pleiotropic effects and strong growth impairment (Portnoy et al., 2011; Mello-de-Sousa et al., 2014), whereas in *T. harzianum* P49P11, it can increase the expression levels of CAZyme genes and *xyr1* (Delabona et al., 2021).

Although *T. harzianum* strains have shown high cellulolytic activity (Horta et al., 2018; Li J. X. et al., 2020), most studies investigating this species have focused on biological control (Maruyama et al., 2020; Yan and Khan 2021). Thus, the regulatory mechanisms underlying hydrolytic enzyme production by these fungi are still poorly explored at the transcriptional level (Delabona et al., 2017; Delabona et al., 2020; Delabona et al., 2021). In addition, given the high degree of genetic variation observed within the genus *Trichoderma* (Kubicek et al., 2019) along with the complex speciation observed in the *T. harzianum* species (Druzhinina et al., 2010), it is necessary to explore how the main regulators XYR1 and CRE1 behave across *T. harzianum* strains.

Previously, the transcriptomes of *T. harzianum* IOC-3844 (Th3844), *T. harzianum* CBMAI-0179 (Th0179), and *T. atroviride* CBMAI-0020 (Ta0020) were investigated under cellulose degradation conditions (Almeida et al., 2021). Different types of enzymatic profiles were reported, and both *T. harzianum* strains had higher cellulase activity than *T. atroviride*. Using this dataset, we aimed to investigate how the regulation of the TFs CRE1 and XYR1 varies among *T. harzianum* strains. Based on the assumption that coexpressed genes tend to share similar expression patterns and that they could be coregulated by the same elements, we modeled a network of Th3844, Th0179, and Ta0020 using a weighted correlation network analysis (WGCNA) (Langfelder and Horvath 2008). The last strain, which is distantly related to *T. reesei* (Druzhinina et al., 2006) and represents a well-defined phylogenetic species (Dodd et al., 2003), was used to assess the differences across *Trichoderma* species. In addition, phylogenetic

analyses of XYR1 and CRE1 protein sequences were performed to clarify the evolutionary relationships of these regulators among the evaluated strains.

In this study, we identified and compared modules, hub genes, and metabolic pathways associated with CRE1 and XYR1 under cellulose degradation conditions. To deeply investigate their regulatory activities, we also performed first neighbor and shortest-path network analyses. Although the evaluated *T. harzianum* strains are phylogenetically close, by comparing their coexpressed transcript profiles, functional diversity was observed. This difference was accentuated when associating the results of Th0179 and Th3844 with those of Ta0020. Thus, we observed a specific transcriptional pattern related to CRE1 and XYR1 in each strain. Our study could contribute to improving our understanding of the regulation of cellulose degradation in *T. harzianum* and paves the way for further studies evaluating differences across strains within the same species. Addressing these questions by investigating the genetic regulatory mechanisms involved in cellulose degradation is important for enhancing both our basic understanding and biotechnological industrial applications of fungal abilities.

## 2 MATERIALS AND METHODS

### 2.1 Fungal Strains, Culture Conditions and Transcription Profiling

The species were obtained from the Brazilian Collection of Environment and Industry Microorganisms (CBMAI) located in the Chemical, Biological, and Agricultural Pluridisciplinary Research Center (CPQBA) of the University of Campinas (UNICAMP), Brazil. The identity of the *Trichoderma* isolates was authenticated by CBMAI based on phylogenetic studies of their internal transcribed spacer (ITS) region and translational elongation factor 1 (*tef1*) marker gene. The *T. harzianum* CBMAI-0179 (Th0179), *T. harzianum* IOC-3844 (Th3844), and *T. atroviride* CBMAI-0020 (Ta0020) strains were cultivated in simple carbon sources, including cellulose and glucose, to induce a clear genetic response. Details on the culture conditions and transcription profiling of the described experiments are provided in **Supplementary Material S1**, while the profile of enzymatic activities (cellulase, beta-glucosidase, and xylanase), the total protein content, and the constitution of the secreted proteome has been published previously (Horta et al., 2018; Almeida et al., 2021).

### 2.2 Phylogenetic Analyses

The ITS nucleotide sequences of *Trichoderma* spp. were retrieved from the NCBI database (<https://www.ncbi.nlm.nih.gov/>). Additionally, ITS nucleotide sequences amplified from the genomic DNA of Th3844, Th0179, and Ta0020 *via* PCR were kindly provided by the CBMAI and included in the phylogenetic analysis. The ITS region has been found to be among the markers with the highest probability of correctly identifying a very broad group of fungi (Schoch et al., 2012). *T. harzianum* T6776 was used as a reference genome to retrieve the CRE1 and XYR1 protein sequences belonging to *Trichoderma* spp. Additionally,

the CRE1 and XYR1 sequences were obtained from the *T. harzianum* T6776 (Baroncelli et al., 2015) reference genome of Th3844 and Th0179 and the *T. atroviride* IMI206040 (Kubicek et al., 2011) genome of Ta0020 and used as references for the TF consensus sequences for RNA-Seq read mapping. These sequences were included in the phylogenetic analyses.

The multiple sequence alignment was performed using ClustalW (Thompson et al., 1994), and a phylogenetic tree was created using Molecular Evolutionary Genetics Analysis (MEGA) software v7.0 (Kumar et al., 2016). The maximum likelihood (ML) (Jones et al., 1992) method of inference was used based on (I) a Kimura two-parameter (K2P) model (Kimura 1980), (II) a Dayhoff model with frequencies (F<sup>+</sup>), and (III) a Jones-Taylor-Thornton (JTT) model for ITS, CRE1, and XYR1, respectively. We used 1,000 bootstrap replicates (Felsenstein 1985) in each analysis. The trees were visualized and edited using Interactive Tree of Life (iTOL) v6 (<https://itol.embl.de/>).

### 2.3 Weighted Gene Coexpression Network Analysis

The gene coexpression networks of Th3844, Th0179, and Ta0020 were modeled using transcripts per million (TPM) value data, which were validated through qPCR and described by Almeida et al. (2021), of three biological replicates with the R (R Core Team 2018) WGCNA package. Transcripts showing null values for most replicates under different experimental conditions were excluded. The network was assembled by calculating the Pearson's correlation coefficient of each pair of genes. A soft power  $\beta$  was chosen for each network using *pickSoftThreshold* to fit the signed network to a scale-free topology. Then, an adjacency matrix in which the nodes correspond to transcripts and the edges correspond to the strength of their connection was obtained. To obtain a dissimilarity matrix, we built a topological overlap matrix (TOM) as implemented in the package.

To identify groups of transcripts densely connected in the gene coexpression network, we applied simple hierarchical clustering to the dissimilarity matrix. From the acquired dendrogram, the *dynamicTreeCut* package (Langfelder et al., 2008) was used to obtain the ideal number of groups and the respective categorization of the transcripts. According to the functional annotation performed by Almeida et al. (2021), groups containing the desired TFs XYR1 and CRE1 were identified and named the *xyr1* and *cre1* groups, respectively.

### 2.4 Functional Annotation of Transcripts in the *xyr1* and *cre1* Groups

We functionally annotated the transcripts in the *xyr1* and *cre1* groups. By conducting a Fisher's exact test to extract the overrepresented terms ( $p$ -value < 0.05), all identified Gene Ontology (GO) (Ashburner et al., 2000) categories were used to identify enriched GO terms with the topGO package in R (Alexa and Rahnenfuhrer 2021). To visualize the possible correlated enriched categories in the dataset caused by cellulose degradation, we created a treemap using the REVIGO

tool (Supek et al., 2011). Then, the metabolic pathways related to the Kyoto Encyclopedia of Genes and Genomes (KEGG) (Kanehisa and Goto 2000) Orthology (KO) identified in *T. reesei* were selected due the high number of annotations correlated with this species in the KEGG database. To identify the pathways related to the enzymes identified as belonging to different groups, we used the Python 3 programming language (Sanner 1999) along with the BioPython library (Cock et al., 2009). The automatic annotation was manually revised using the UniProt databases (UniProt Consortium 2019).

## 2.5 Assessing the Groups' Network Topologies

To provide a visual network characterization, we modeled additional gene coexpression networks of all strains using the highest reciprocal rank (HRR) approach (Mutwil et al., 2010). Using an R Pearson correlation coefficient threshold of 0.8, we assessed the 30 strongest edges, which were coded as  $\infty$  (top 10), 1/15 (top 20), and 1/30 (top 30). To visualize the behavior of the groups modeled by WGCNA in the HRR networks, we used Cytoscape software v3.7.0 (Shannon et al., 2003). Using the HRR methodology, we were able to infer the possible biological correlations depending on the network topology. First, by performing a topological analysis based on the degree distribution, we identified and compared the hub nodes in the *cre1* and *xyl1* groups among all evaluated strains. Second, to identify the more indirect associations of both TFs studied, we considered HRR global networks to evaluate the first neighbors of the *xyl1* and *cre1* transcripts. Finally, because XYR1 and CRE1 are described as regulatory proteins in CAZyme gene expression, we were also interested in evaluating the minimum pathway between these regulatory proteins and these hydrolytic enzymes. Based on the classification proposed by Almeida et al. (2021), we selected CAZymes with higher expression levels under cellulose growth conditions (upregulated transcripts) that were present in both Th0179 and Th3844. To obtain the corresponding homologs of Ta0020, BLASTp was performed using *T. atroviride* IMI206040 as the reference genome. The numbers of the shortest paths between both TFs, namely, CRE1 and XYR1, and the selected CAZymes were identified using the Pesca v. 3.0 plugin (Scardoni et al., 2016) in Cystoscape. The results were visualized using the R package pheatmap (Kolde 2019).

## 3 RESULTS

### 3.1 Molecular Phylogeny of the Evaluated *T. harzianum* Strains

Although Kubicek et al. (2019) deeply investigated the phylogenetic relationships in the genus *Trichoderma*, no results were reported for Th3844, Th0179, and Ta0020. Here, we modeled a phylogenetic tree based on the ITS sequence of 14 *Trichoderma spp.*, including those of our study strains (Supplementary Figure S1). According to the results, high genetic proximity between Th3844 and Th0179 was observed. In contrast, both strains were phylogenetically distant from

Ta0020, which grouped with other *T. atroviride* strains. *Neurospora crassa* and *Fusarium oxysporum* were used as outgroups.

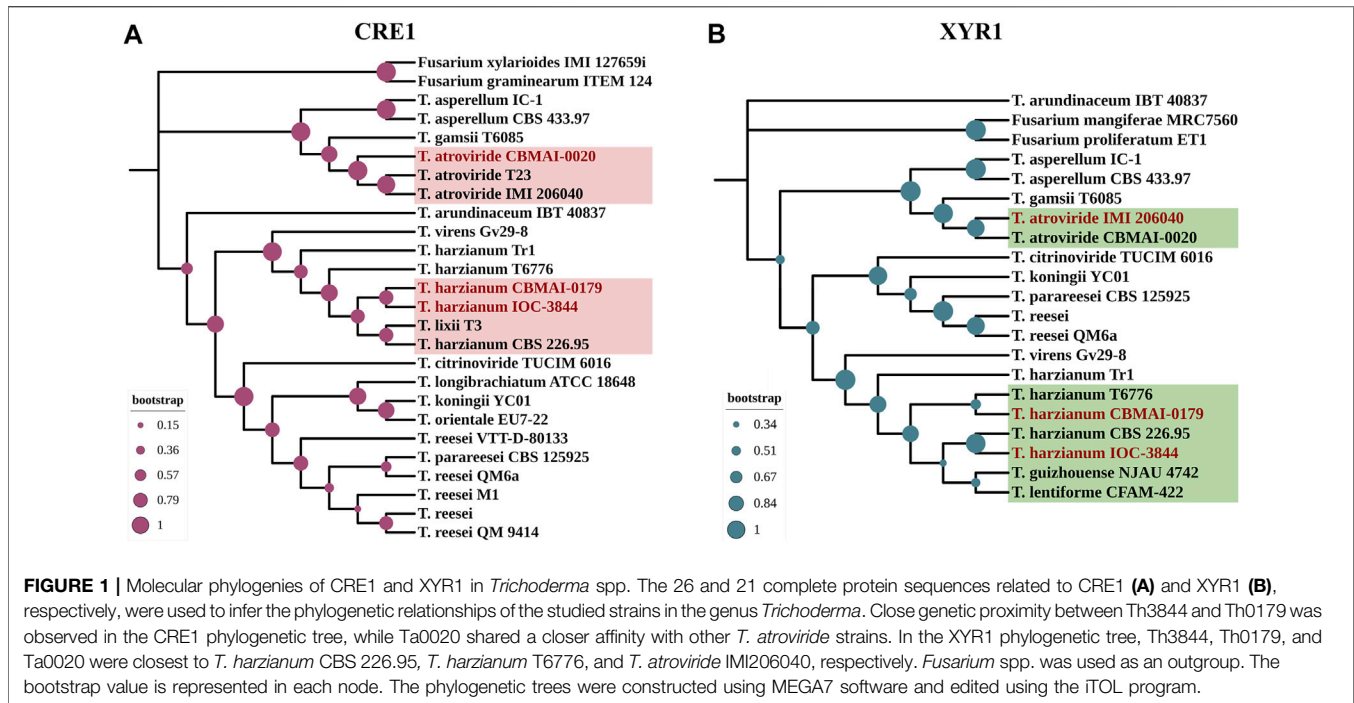
Additionally, to represent the evolutionary relationships of CRE1 and XYR1 among Th3844, Th0179, and Ta0020, a phylogenetic analysis was performed while considering their amino acid sequences (Figure 1). The phylogenetic trees were modeled based on 26 and 21 protein sequences related to CRE1 and XYR1, respectively, in the *Trichoderma* genus, including those of our studied strains. *Fusarium spp.* was used as an outgroup. The NCBI accession number of the sequences used to model the phylogenetic trees is available in Supplementary Table S2.

The CRE1 phylogenetic tree indicated a close genetic proximity between Th3844 and Th0179 (with bootstrap support of 67%) (Figure 1A). These results were supported by the alignment of both protein sequences, which showed high conservation in the alignment of their amino acid sequences (with a percent identity of 99.76%) (Supplementary Figure S2). In contrast, the CRE1 protein sequence of Ta0020 shared closer affinity with two other *T. atroviride* strains (T23 and IMI206040), with bootstrap support of 99% (Figure 1A). Furthermore, the C<sub>2</sub>H<sub>2</sub> domain is highly conserved in the Th3844, Th0179, and Ta0020 sequences of CRE1, with only one amino acid change from *T. atroviride* compared to both *T. harzianum* strains (Supplementary Figure S2).

In the XYR1 phylogenetic tree, Th3844, Th0179, and Ta0020 were closest to *T. harzianum* CBS 226.95 (with bootstrap support of 97%), *T. harzianum* T6776 (with bootstrap support of 51%), and *T. atroviride* IMI206040 (with bootstrap support of 88%), respectively (Figure 1B). Compared to the results of CRE1, the alignment of their amino acid sequences showed a lower percentage of identity, supporting the phylogenetic results observed (Supplementary Figure S2). In addition, the multiple alignments of the XYR1 protein sequence of Th3844, Th0179, and Ta0020 showed reasonable conservation of the Zn2Cys6 and fungal-specific TF domains (Supplementary Figure S2).

### 3.2 Weighted Gene Coexpression Network Analysis

Recently, the transcriptomes of Th3844, Th0179, and Ta0020 grown on crystalline cellulose and glucose after a time course of 96 h were investigated (Almeida et al., 2021). By using these transcriptome data and applying the described filters in the WGCNA package, we obtained (I) 11,050 transcripts (Th3844), (II) 11,105 transcripts (Th0179), and (III) 11,021 transcripts (Ta0020) (Supplementary Table S3). Based on these transcripts, we calculated Pearson's correlation matrices. Then, different soft power  $\beta$  values were chosen (48 for Th3844, 8 for Th0179, and 27 for Ta0020) to obtain the scale-free topology, reaching fit indexes of (I) 0.8 for Th3844 (mean connectivity of 40), (II) 0.9 for Th0179 (mean connectivity of 842), and (III) 0.85 for Ta0020 (mean connectivity of 406). Then, the networks were partitioned into manageable groups to explore the putative coregulatory relationships. In total, we identified 87 groups in



Th3844, 75 groups in Th0179, and 100 groups in Ta0020 (Supplementary Table S4). Transcripts with expression patterns correlated with XYR1 and CRE1 were identified in the Th3844, Th0179, and Ta0020 coexpression networks and grouped (described in Supplementary Table S5). Among the strains, Ta0020 presented the highest number of transcripts coexpressed with *cre1* and the lowest number of transcripts coexpressed with *xyr1*; the other strains showed the opposite profile.

### 3.3 Functional Characterization of the Transcripts in the *xyr1* and *cre1* Groups

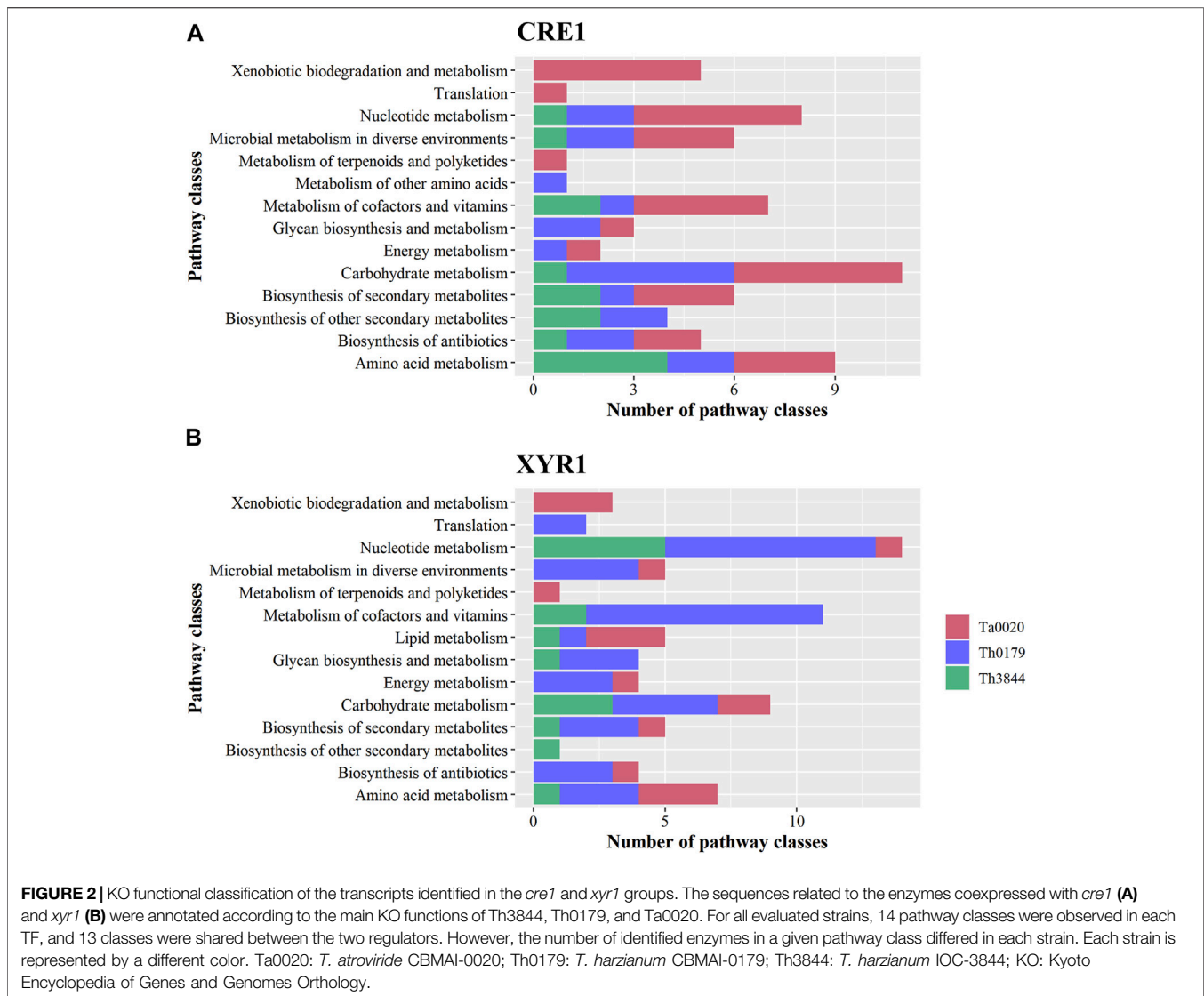
We performed an enrichment analysis of the transcripts in each *cre1* and *xyr1* group of all evaluated strains using the GO categories (Supplementary Figures S3–S5, respectively). The *cre1* group of Th3844, Th0179, and Ta0020 presented 50, 38, and 50 enriched GO terms, respectively, while in the *xyr1* group, 34, 86, and 50 enriched GO terms were found in Th3844, Th0179, and Ta0020, respectively. Overall, the GO terms describing the transcripts of these groups were diverse across all strains, indicating a high degree of differences among the biological processes related to XYR1 and CRE1.

For example, the enrichment analyses of Ta0020 indicated that the carbohydrate metabolic process might be directly affected by CRE1 (high percentage of enriched GOs). Furthermore, GO terms related to fungal growth and nucleoside transmembrane transport were observed. In contrast, in Th0179 and Th3844, organic substance metabolic processes and regulation processes were pronounced, respectively. Interestingly, response to light stimulus was an enriched GO term in the *cre1* group of Th3844, and fungal-type cell wall organization was an enriched GO term

in Th0179. In the XYR1 group, Ta0020 also presented carbohydrate metabolic process as an enriched GO term. However, few genes corresponding to this term were observed, while terms related to the regulation of DNA transcription were pronounced. Interestingly, response to external stimulus and oxidation-reduction process were notable terms in Th0179 and Th3844, respectively. Furthermore, our results suggest that the regulation of biological processes was a common enriched term in all the evaluated strains, with some particularities across the *T. harzianum* strains, including regulation of cell population proliferation (Th0179) and mRNA metabolic process (Th3844).

The KO functional annotation of the transcripts encoding enzymes and unknown proteins with enzymatic activity in the *cre1* and *xyr1* groups was also investigated. In the 14 pathway classes observed in each TF, 13 were shared between the two regulators (Figure 2). Only two pathway classes, i.e., metabolism of other amino acids and lipid metabolism, were exclusive to CRE1 and XYR1, respectively. However, the number of identified enzymes in a given pathway class differed in each strain. This difference stresses the diversity of proteins with several functions, which could result in exclusive enzymatic performance in cellulose degradation according to the strain.

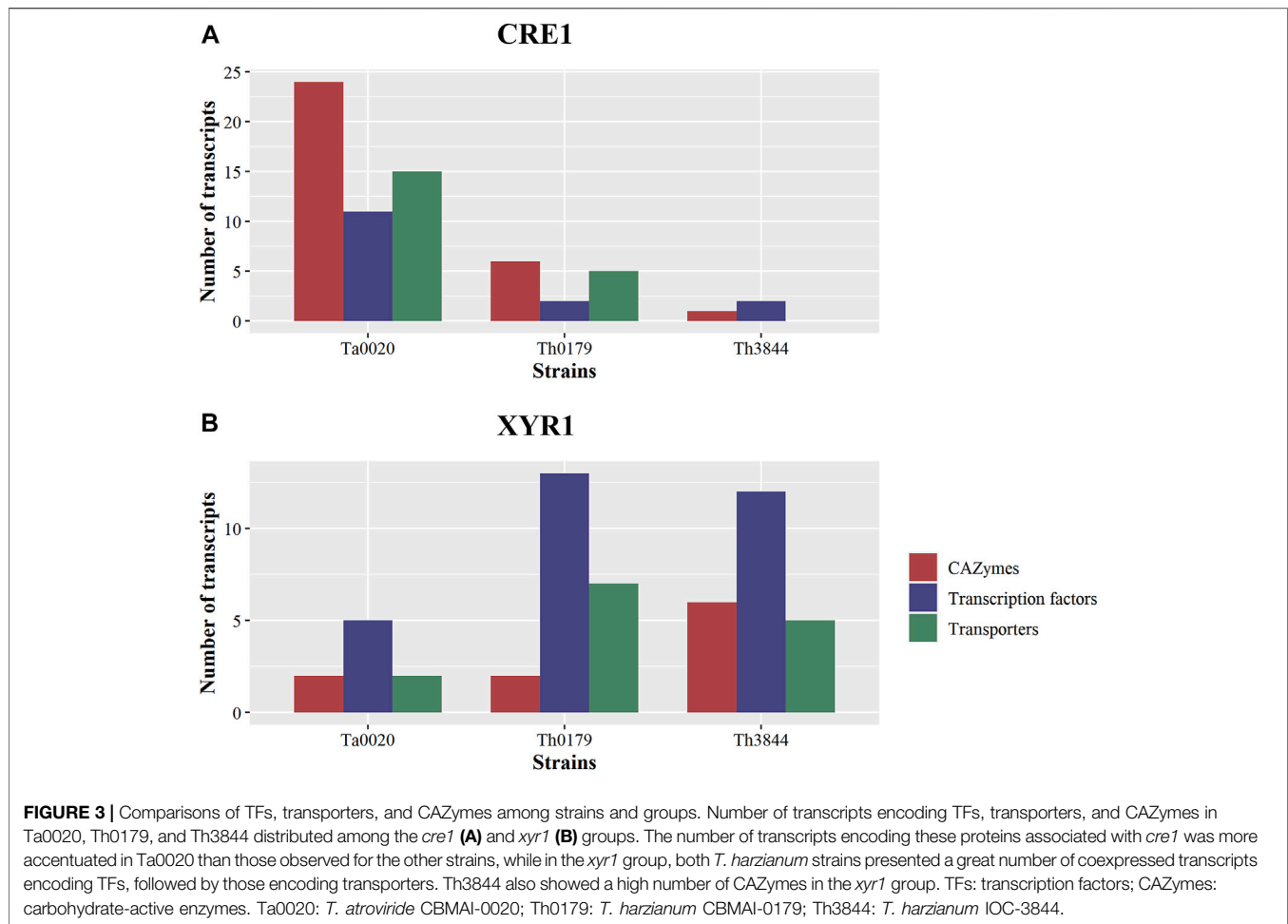
Next, we summarize some important aspects of the identified metabolic pathways. For example, Ta0020 showed a greater number of enriched pathway classes in the *cre1* group, while both *T. harzianum* strains presented the opposite profile, with more enzymatic activity pathways enriched in the *xyr1* group. Carbohydrate metabolism was a pathway class enriched in both *T. harzianum* strains in the *xyr1* group, while Th0179 and Ta0020 presented such a profile in the *cre1* group. In the *xyr1* group, nucleotide metabolism and metabolism of cofactors and vitamins were enriched terms in Th0179, while xenobiotic degradation and



metabolism of terpenoids and polyketides were enriched terms exclusively in Ta0020. The pathway classes related to secondary metabolite compounds were also enriched in all evaluated strains in the *cre1* and *xyr1* groups, and Ta0020 presented the highest number of enzymes related to this term in the *cre1* group.

In this study, network analyses were conducted to investigate how the molecular basis of XYR1 and CRE1 for cellulose-degrading enzyme production varies among *T. harzianum* strains. Thus, after analyzing the functional composition of the transcripts in the *cre1* and *xyr1* groups of all evaluated strains, particular attention was given to CAZymes, TFs, and transporters (Figure 3). We observed that in the *cre1* group, Ta0020 showed the highest number of transcripts encoding CAZymes, TFs, and transporters, while in the *xyr1* group, both *T. harzianum* strains presented a great number of coexpressed transcripts encoding TFs, followed by those encoding transporters. Furthermore, Th3844 showed a high number of CAZymes in the *xyr1* group.

We identified the main CAZyme classes, including glycoside hydrolases (GHs), carbohydrate esterases (CEs), glycosyltransferases (GTs), and polysaccharide lyases (PLs) Lombard et al., 2014, coexpressed with *xyr1* and *cre1* transcripts. To determine the similarities and differences across the strains, their CAZyme profiles were compared (Figure 4). In the *xyr1* and *cre1* groups, the GH family, which encompasses enzymes that hydrolyze glycosidic bonds, was identified in all the evaluated strains with different numbers of transcripts (Figures 4A,B). In the *cre1* group, Ta0020 presented the highest number of classified transcripts of the GH family, followed by Th0179 and Th3844. In the *xyr1* group, Th3844 presented a higher number of GHs than Th0179 and Ta0020. Furthermore, transcripts encoding CEs, which hydrolyze ester bonds, were associated with the *cre1* transcript in Ta0020 and Th0179, whereas transcripts of the PL family, which cleave bonds in uronic acid-containing polysaccharide chains, were

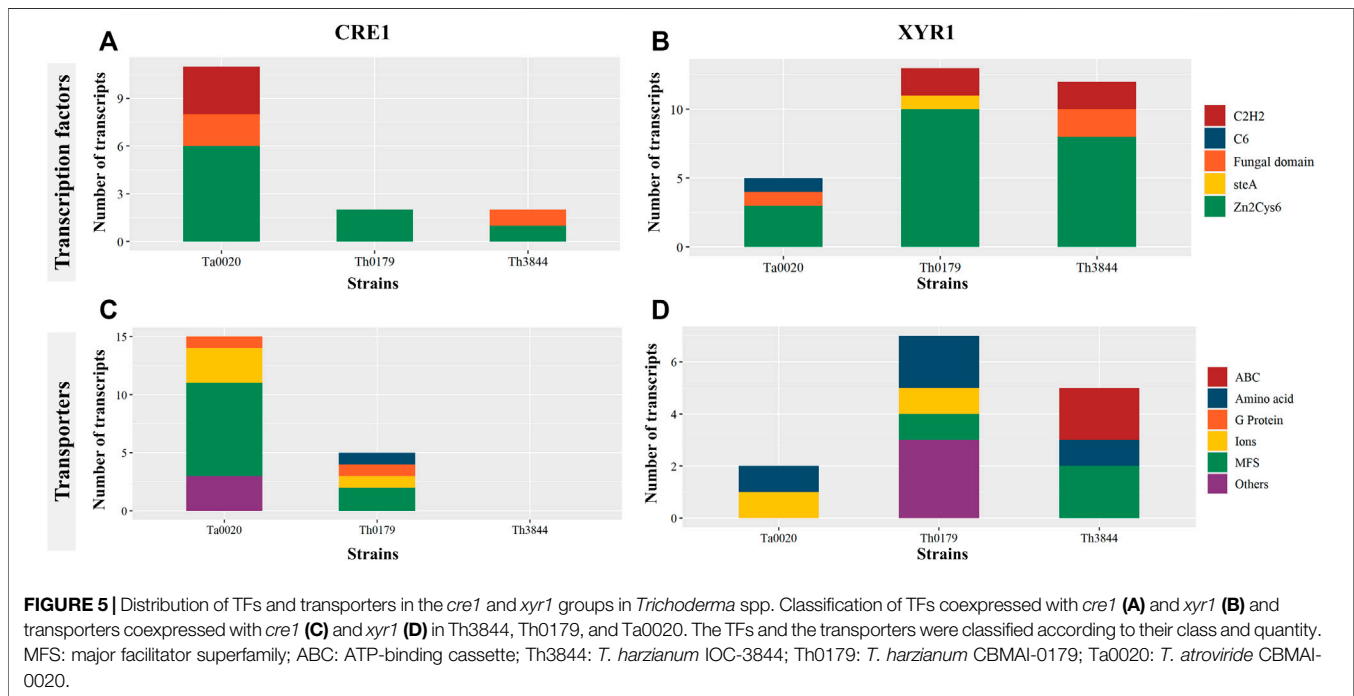
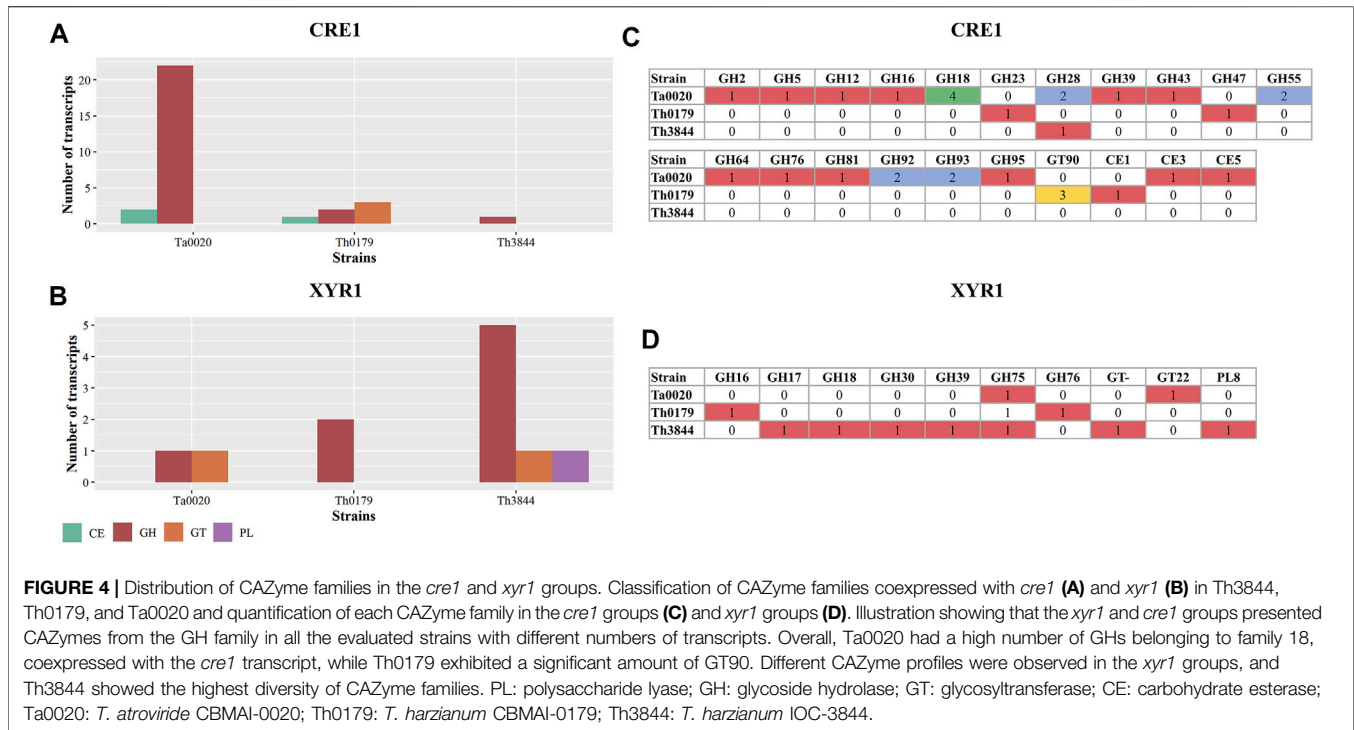


coexpressed with the *xyr1* transcript in only Th3844. In addition, transcripts of the GT family, which synthesizes glycosidic bonds from phosphate-activated sugar donors, were present in the *cre1* group of Th0179 and the *xyr1* groups of Th3844 and Ta0020. We also investigated the quantification of each CAZyme family in the *cre1* and *xyr1* groups of all evaluated strains (Figures 4C,D). Overall, Ta0020 presented a high number of GHs belonging to family 18, coexpressed with the *cre1* transcript, while Th0179 exhibited a significant amount of GT90 (Figure 4C). Different CAZyme profiles were observed in the *xyr1* groups, and Th3844 showed the highest diversity of CAZyme families (Figure 4D).

Several positive and negative regulators are involved in the expression of CAZyme-coding genes and other proteins required for lignocellulose breakdown. Thus, we sought to identify transcripts encoding TFs coexpressed in the *cre1* and *xyr1* groups (Figure 5). In both groups, transcripts encoding Zn<sub>2</sub>Cys<sub>6</sub>-type TFs were identified in all the evaluated strains with different numbers of transcripts. In the *cre1* group of Ta0020, the number was higher than that observed in Th0179 and Th3844 (Figure 5A), while in the *xyr1* group, we observed the opposite profile (Figure 5B). Most Zn<sub>2</sub>Cys<sub>6</sub> proteins also contain a fungal-specific TF domain, which was coexpressed

with both *cre1* and *xyr1* transcripts in Th3844 and Ta0020. In this last strain, a C6 zinc finger domain TF was coexpressed with *xyr1*. Transcripts encoding C<sub>2</sub>H<sub>2</sub>-type TFs were identified in Ta0020 and *T. harzianum* strains in the *cre1* and *xyr1* groups, respectively. Furthermore, in the *xyr1* group, we found a transcript encoding the SteA regulator, which is involved in the regulation of fungal development and pathogenicity (Hoi and Dumas 2010), in Th0179.

Transporters are also important players in the degradation of plant biomass. Here, transcripts encoding transport proteins coexpressed with *cre1* and *xyr1* were selected (Figure 5). Among them, transcripts encoding major facilitator superfamily (MFS) transport proteins were coexpressed with *cre1* in Th0179 and Ta0020 (Figure 5C) and *xyr1* in Th0179 and Th3844 (Figure 5D). Amino acid transporters were present in the *xyr1* groups of all strains and the *cre1* group only of Th0179. Transcripts encoding the ATP-binding cassette (ABC) were coexpressed with *xyr1* only in Th3844. Th0179 showed transcripts encoding several types of transporters coexpressed with *xyr1*, e.g., vesicle transporter SEC22, cation transporting ATPase, and calcium-dependent mitochondrial carrier, while Ta0020 coexpressed with *cre1*, e.g., UDP-galactose transporter and concentrative nucleoside

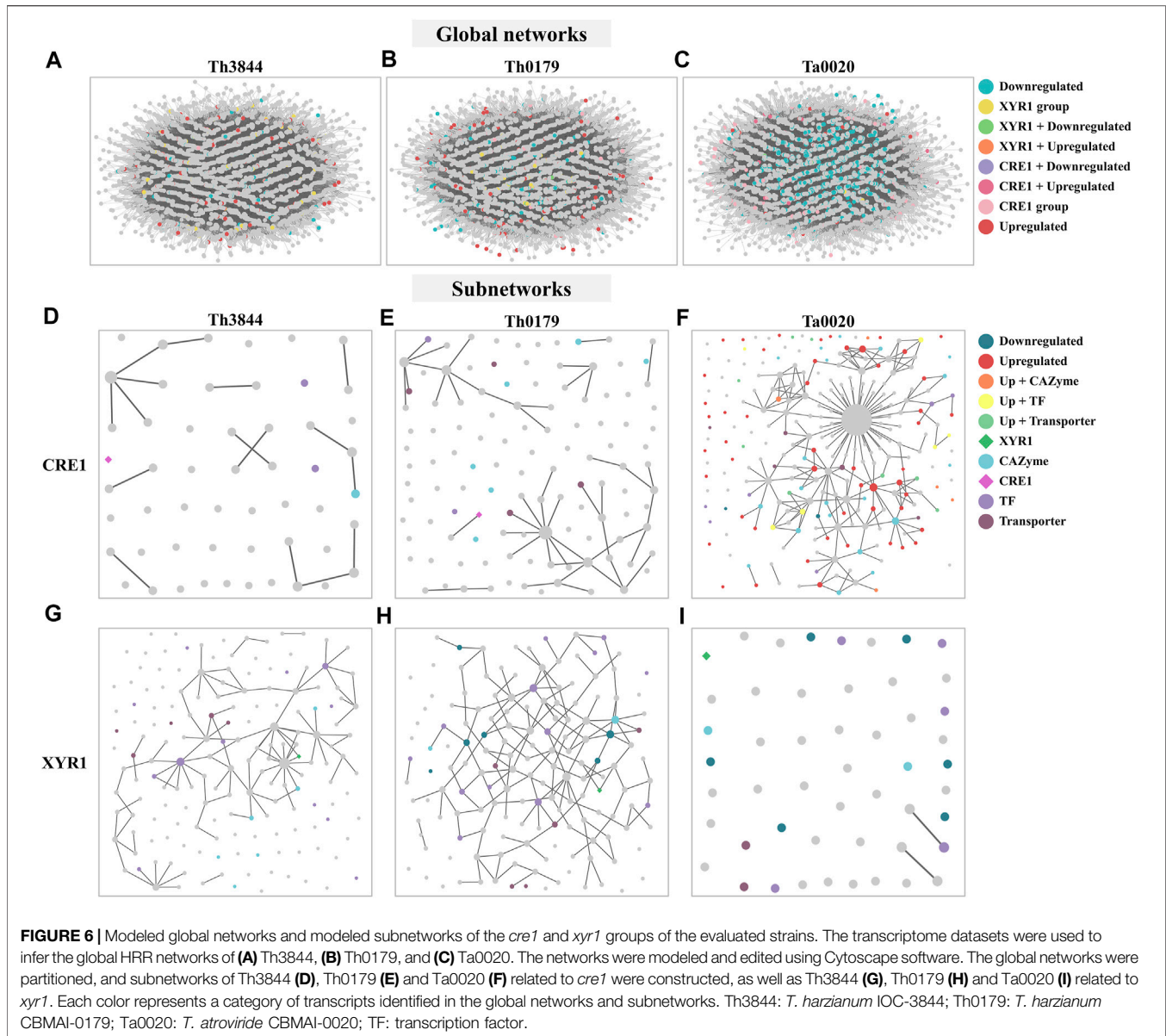


transporter (CNT). Transcripts encoding ion transporters were present in both the *cre1* and *xyr1* groups of Ta0020 and Th0179. In the *cre1* group, such transcripts included zinc and magnesium transporter proteins in Ta0020 and potassium transporter proteins in Th0179. In the *xyr1* group, such transcripts include  $\text{Cd}^{2+}\text{Zn}^{2+}$  transporters in Ta0020 and

$\text{Ca}^{2+}$  transporters in Th0179. Th0179 and Th3844 also present a G protein coexpressed with the *cre1* transcript.

To better understand the regulation mediated by the studied TFs in the evaluated *T. harzianum* strains, we also investigated other classes of proteins coexpressed with the *cre1* and *xyr1* transcripts. For example, phosphatases, kinases and TFs are key





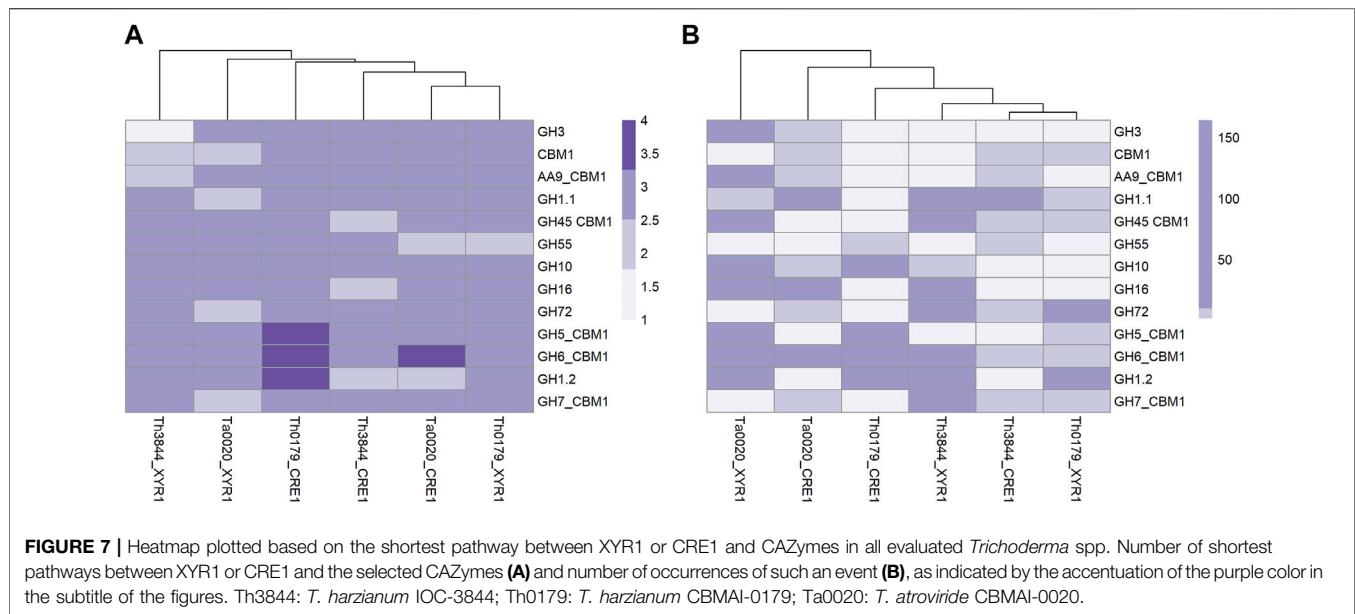
components in cellular signaling networks. Transcripts encoding kinase proteins were coexpressed with *cre1* transcripts in Ta0020 and Th3844 and *xyr1* transcripts in Ta0020 and Th0179. In addition, all strains showed transcripts encoding phosphatases coexpressed with *cre1*, and in Th0179 and Th3844, such transcripts were coexpressed with *xyr1*. In addition, transcripts encoding cytochrome P450 genes, which constitute an important group of enzymes involved in xenobiotic degradation and metabolism, were found in the *cre1* groups of all the evaluated strains.

Furthermore, different quantities of differentially expressed transcripts were found in Ta0020 (78) and Th0179 (6) (described in **Supplementary Tables S6, S7**). In Ta0020, most upregulated transcripts under cellulose growth (70) were associated with the *cre1* group, including *cre1*, whereas *xyr1* demonstrated a potentially significant expression level under glucose growth.

In Th3844, *cre1* significantly modulated the expression of the two carbon sources, with a high expression level under glucose growth. Even with the reduced differentiation observed ( $-1.13$ ), this phenomenon was considered in other studies (Antonieto et al., 2014; Castro et al., 2016). In Th0179, *xyr1* and *cre1* revealed a low modulation in transcript expression between growth under cellulose or glucose. However, *xyr1* had a higher transcript expression level under glucose than *cre1*, which had a higher transcript expression level under cellulose growth conditions. In Th3844, *xyr1* exhibited similar results.

### 3.4 Assessing the Groups' Network Topologies

To identify the main aspects of the network topologies, we applied the HRR methodology to the transcriptome data,



which were also used to model the networks using the WGCNA methodology (Figures 6A–C).

In the CRE1 and XYR1 subnetworks, different connection profiles were observed in each strain. While the transcripts in the *cre1* groups showed less ranked connections in the WGCNA groups of the *T. harzianum* strains (Figures 6D,E), Ta0020 showed the opposite profile. In this strain, the transcripts in the *cre1* group were more strongly connected (Figure 6F). In contrast, in the *xyr1* groups, the transcripts were more densely connected in the *T. harzianum* strains (Figures 6G,H), while in Ta0020, the transcripts were separated (Figure 6I).

Transcripts at the top of the degree distribution, which are defined here as hubs, are topologically important to the network structure and are often functionally relevant (Luscombe et al., 2004). Thus, the hub nodes were sought in the *cre1* and *xyr1* groups. In the *cre1* groups, transcripts encoding a SET-domain protein, an ATP synthase, and a transcript not yet annotated were hub nodes of Th3844, Th0179, and Ta0020, respectively. In Ta0020, we found that such an uncharacterized transcript had a degree value equal to 52, which differs from the *T. harzianum* strains in which the hub nodes had degree values of 4 (Th3844) and 9 (Th0179) (Supplementary Table S8). In the *xyr1* groups, transcripts encoding an ATP-dependent RNA helicase, a cytokinesis *sepA*, and hypothetical proteins were found as hub nodes of Th3844, Th0179, and Ta0020, respectively (Supplementary Table S8). Here, we show that the hub nodes in the *cre1* group of Ta0020 had a degree value of 1 and all encoded hypothetical proteins, while in the *T. harzianum* strains, the hub nodes had degree values of 13 (Th3844) and 7 (Th0179). Among the other transcripts with a degree value lower than that of those at the top of the degree distribution, in the *xyr1* group, GH76 and Zn<sub>2</sub>Cys<sub>6</sub>-type TFs (degree value of 6) were identified as candidate hub genes of Th0179, while regulator-nonsense transcripts (degree value of 9) and Zn<sub>2</sub>Cys<sub>6</sub>-type TFs (degree value of 8) were identified as candidate hub genes of Th3844. In the *cre1*

group, the proteasome component PRE3 (degree value of 2) in Th3844 was found as a hub node, and replication factor C and phosphoglucomutase (degree value of 5) were found in Th0179. In addition, in Ta0020, we identified calcium calmodulin-dependent kinase (degree value of 9) and GH93 (degree value of 8) as hub nodes.

In all evaluated strains, as a reduced number of differentially expressed transcripts was found in the *cre1* and *xyr1* groups, we expanded our investigation of the studied groups by selecting the first neighbors of XYR1 and CRE1 in global HRR networks. Different quantities of *cre1* neighbors were found in Th3844 (59), Th0179 (21), and Ta0020 (25), and different quantities of *xyr1* were found in Th3844 (46), Th0179 (59), and Ta0020 (70) (described in Supplementary Table S9). Regarding the *cre1* neighbors, these transcripts were distributed among 24 groups in Th3844, 15 groups in Th0179, and 16 groups in Ta0020. In contrast, considering the *xyr1* neighbors, such transcripts were distributed among 19 groups in Th3844, 32 groups in Th0179, and 42 groups in Ta0020. The direct coexpressed neighbors of *xyr1* included downregulated transcripts in Th3844 (4), Th0179 (5), and Ta0020 (22) and upregulated transcripts in Th3844 (1), Th0179 (1), and Ta0020 (1). Interestingly, only Ta0020 showed differentially expressed transcripts as the first neighbor of the *cre1* transcript (4 downregulated and 4 upregulated). Overall, these differentially expressed transcripts included transporters, CAZymes, kinases, and other proteins related to the regulation process.

For simplification, only a few neighboring transcripts of *xyr1* and *cre1* in Th3844, Th0179, and Ta0020 are shown in Table 1. In Th3844, TFs, transporters, a cytochrome, and a phosphatase were found to be first neighbors of the *cre1* transcript, while TFs, transporters, and CAZymes were found to be the first neighbors of the *xyr1* transcript. In Th0179, several types of proteins, including a kinase, were found to be first neighbors of *cre1*, while transporters, CAZymes, and a TF were found to be first neighbors of the *xyr1* transcript. In Ta0020, several types

**TABLE 1 |** First neighbors of the transcripts *xyr1* and *cre1* identified in Th3844, Th0179, and Ta0020.

First neighbors					
Th3844					
CRE1			XYR1		
Gene ID	Description	Group	Gene ID	Description	Group
THAR02_06363	Zn2Cys6 transcriptional regulator	29	THAR02_07076	regulator-nonsense transcripts 1	9
THAR02_10232	phosphate:H+ symporter	13	THAR02_00049	polysaccharide lyase family 7	11
THAR02_07487	Mg2+ transporter	78	THAR02_09951	MFS permease	70
THAR02_07586	cytochrome P450 CYP2 subfamily	39	THAR02_01555	MFS permease	0
THAR02_07548	C2H2 transcriptional regulator	13	THAR02_00890	glycoside hydrolase family 3	0
THAR02_04042	acid phosphatase	8	THAR02_09118	fungal specific transcription factor	26
<b>Th0179</b>					
THAR02_03655	proteasome subunit alpha type-5	70	THAR02_00084	MFS transporter	63
THAR02_06292	restriction of telomere capping 5	53	THAR02_02333	MFS transporter	30
THAR02_11314	xaa-Pro aminopeptidase	46	THAR02_11077	glycosyltransferase family 2	35
THAR02_03482	kinase domain	32	THAR02_00098	glycoside hydrolase family 43	67
THAR02_03668	adenine phosphoribosyltransferase	31	THAR02_03812	G-coupled receptor	39
THAR02_00283	NADH dehydrogenase	8	THAR02_04897	C2H2 transcriptional regulator	19
<b>Ta0020</b>					
013948456.1_10935	SH3 domain-containing	52	013943820.1_6616	Zn2Cys6 transcriptional regulator	14
013938015.1_374	serine threonine kinase	7	013943207.1_5652	replication factor A1	17
013937789.1_299	ribosomal S18	35	013941180.1_3604	MFS transporter	1
013949023.1_11526	pleiotropic drug resistance	2	013943062.1_5470	MFS transporter	90
013946760.1_9261	MYB DNA-binding domain-containing	13	013941580.1_4080	glycoside hydrolase family 76	1
013941398.1_3866	aspartate aminotransferase	28	013945761.1_8223	DNA ligase 1	16

of proteins, including kinases, were found to be first neighbors of *cre1*, while transporters, CAZymes, TFs, and a DNA ligase were found to be first neighbors of the *xyr1* transcript. Hypothetical proteins were also found to be neighbors of the *cre1* and *xyr1* transcripts of all strains, indicating that both regulators might have a regulatory influence on uncharacterized proteins.

We also applied a shortest-path network analysis to identify possible transcripts outside of the *xyr1* and *cre1* groups that may be influenced by CRE1 and XYR1 (described in **Supplementary Table S10**). As the shortest path, we considered the minimal number of edges that need to be traversed from a node to reach another node (Koutrouli et al., 2020). As both regulators act on the gene expression of hydrolytic enzymes related to plant biomass degradation, we sought to determine the number of shortest paths from XYR1 and CRE1 to the selected CAZymes. In all evaluated strains and both TFs, we found a similar quantity of shortest paths (**Figure 7A**; **Supplementary Figures S6, S7**). However, some aspects should be noted. For example, Th0179 presented transcripts encoding CAZymes from the GH1, GH5, and GH6 families, which are more distantly related to CRE1, while Ta0020 showed only a CAZyme from the GH6 family satisfying this requirement. In Th3844, we found a transcript encoding a CAZyme from GH3 strongly related to XYR1, and CAZymes with the CBM1 domain were also closely connected with such a regulator. In Th0179, a CAZyme from GH5 exhibited a close relationship with XYR1, while in Ta0020, CAZymes from the GH7, GH72, and GH1 families and the CBM1 domain also presented such a profile. In addition, given a determined shortest path, we also considered the number of possibilities that may have occurred (**Figure 7B**; **Supplementary**

**Figures S6, S7**). Across all strains and in both TFs, significant differences were observed in the number of chances. For instance, a significant number of possible minimum paths between CRE1 and a CAZyme from the GH6 family were observed in Ta0020, likely suggesting a strong influence of this repressor regulator on enzyme activity. Similarly, CAZymes from the AA9 and GH16 families appeared to be affected by XYR1. In Th0179, CAZymes from GH10, GH6, and GH1 presented a higher number of possible shortest paths related to CRE1, potentially indicating an impact of this TF on these enzyme activities.

We also performed a shortest-path analysis to identify transitive transcripts between *cre1* or *xyr1* and the selected CAZymes, which allowed us to discover new transcripts that may be involved in the same biological process. For simplification, we only chose a few shortest paths to explore such transitive transcripts. In Th3844, NADH:ubiquinone oxidoreductase (THAR02\_08259), which is the largest multiprotein complex of the mitochondrial respiratory chain (Whitehouse et al., 2019), was found between GH45 with a CBM1 domain (THAR02\_02979) and *cre1*. We also found another transcript involved in ATP synthesis, NAD(P) transhydrogenase beta subunit (THAR02\_08260), between GH1 (THAR02\_05432) and *cre1*. Furthermore, a transcript encoding a component of the endoplasmic reticulum quality control system called ER-associated degradation (THAR02\_08220) (Phillips et al., 2020) was found between GH16 (THAR02\_03302) and *cre1*. Interestingly, in Ta0020, a phosphotyrosine phosphatase was found in the shortest path between GH1 (TRIATDRAFT\_135426), which is a homolog of GH1 (THAR02\_05432) in *T. harzianum* strains, and *cre1*. This phosphatase is involved in protein phosphorylation, which is a

key posttranslational modification critical for the control of many cellular functions (Nasa and Kettenbach 2018). In Th3844, we found a transcript encoding a mitochondrial outer membrane porin (THAR02\_07078) between CBM1 (THAR02\_02133) and *xyr1*. These protein transporters transport small molecules and play significant roles in diverse cellular processes, including the regulation of mitochondrial ATP and calcium flux (Grevel and Becker 2020). In Ta0020, methyltransferase domain-containing (TRIATDRAFT\_292180), which is important for the regulation of chromatin and gene expression (Kouzarides 2007), was found between GH1 (TRIATDRAFT\_150220) and *xyr1*.

## 4 DISCUSSION

Although the importance of XYR1 and CRE1 in the expression of CAZyme-encoding genes and other proteins required for lignocellulose degradation is evident, the transcriptional regulation mediated by both proteins in *T. harzianum* strains remains poorly explored (Delabona et al., 2017; Delabona et al., 2021). A previous study demonstrated that some genes encoding regulatory proteins, such as *xyr1*, evolved by vertical gene transfer in *Trichoderma* spp. (Druzhinina et al., 2018). Here, we inferred the evolutionary relationships of XYR1 and CRE1 in the evaluated strains. In both regulatory proteins, a great genetic distance was observed between the amino acid sequences of Ta0020 and those of Th3844 and Th0179. These findings supported the genetic tree of the evaluated species in which Ta0020 was grouped with other *T. atroviride* strains. However, among the *T. harzianum* strains, we noted that the CRE1 amino acid sequences were more highly conserved than those of XYR1. These results are consistent with previous studies reporting that while the function of CRE1 is conserved throughout the fungal kingdom (Adnan et al., 2017), the role of XYR1 greatly differs across ascomycete fungi (Klaubauf et al., 2014).

Recently, different types of enzymatic profiles across *Trichoderma* species were reported, and Th3844 and Th0179, which have hydrolytic potential, have higher cellulase activity during growth on cellulose than Ta0020 (Almeida et al., 2021). Because such diversity in the enzyme response can be affected by the specific functionalities of regulatory proteins and evolutionary divergence between XYR1 and CRE1 (Klaubauf et al., 2014; Benocci et al., 2017), we aimed to investigate how both TFs could affect the activities of the transcripts in response to cellulose degradation in the *T. harzianum* strains. Because transcripts that share the same function or are involved in the same regulatory pathway tend to present similar expression profiles and, hence, form modules (Wolfe et al., 2005), networks were modeled for Th3844, Th0179, and Ta0020, and the last strain was used to assess the differences across *Trichoderma* species. In fungi, such methodology has been successfully used to provide insight into the regulatory mechanisms of hydrolysis (Borin et al., 2018; Arntzen et al., 2020; Li C. X. et al., 2020).

In recent years, network methodologies have been employed for the discovery of new targets associated with biological

processes (Cortijo et al., 2020; Liu et al., 2021; Zhang et al., 2021). Because such approaches might provide mechanisms for inferring new gene relationships and functions, experimental validation by the construction of mutants is usually a way of corroborating these insights. In this context, the construction of mutants can show the influence of a unique missing gene on genome regulation, helping to corroborate the hypotheses raised in the present study. However, due to the inefficient homologous recombination machinery of filamentous fungi, once a fungus reproduces asexually, a low frequency of correct genomic integration has been observed for *Trichoderma* spp. (Zeilinger 2004; Liu et al., 2017; Vieira et al., 2018). These challenges can be overcome by using the CRISPR/Cas9 system, which represents a good alternative in *Trichoderma* spp. (Fonseca et al., 2020; Vieira et al., 2021) and may enable the future establishment of efficient protocols for each strain described here. Thus, by predicting the profiles of the transcripts coexpressed with XYR1 and CRE1, the results can be used to engineer mutant strains with the objective to investigate the influence of the regulation of such TFs *in vitro*.

We observed that each network had a different configuration with distinct module profiles of XYR1 and CRE1, providing insight into how these TFs might act in specific ways in different *Trichoderma* species. These functional differences in the *xyr1* and *cre1* groups can be attributed to previously reported differences in the regulatory mechanisms of hydrolysis (Almeida et al., 2021). By analyzing both groups, we observed that more transcripts were coexpressed with XYR1 in the *T. harzianum* strains than *T. atroviride*, which had more transcripts coexpressed with CRE1. However, although the phylogenetic similarity between the evaluated *T. harzianum* strains shows that they share a largely common genetic background, their profiles of transcripts coexpressed with *xyr1* and *cre1* differed.

### 4.1 Insight Into the Genetic Impacts of XYR1 and CRE1

To obtain insight into the functional profile of the *cre1* and *xyr1* groups, GO enrichment analyses of transcripts from these groups of all evaluated strains were performed. Here, response to external stimulus was a notable GO term in Th0179 in the *xyr1* group, suggesting that the transcripts of these group likely respond to external environmental conditions, such as carbon sources. Furthermore, interconnections between nutrient and light signaling pathways have been reported in filamentous fungi, such as *N. crassa* and *T. reesei*, with substantial regulation by photoreceptors (Schmoll 2018). More interestingly, the influence of light on CRE1 functions has been reported (Monroy et al., 2017), supporting our findings showing that the response to a light stimulus was an enriched GO term in the *cre1* group of Th3844. In contrast, the enrichment analysis of Ta0020 indicates that the activity of CRE1 may be stronger in such fungi, directly repressing genes related to plant cell wall-degrading enzymes, which was not observed in the *T. harzianum* strains. In these strains, organic substance metabolic processes (Th3844) and

regulation processes (Th0179) were enriched GO terms. In addition, fungal-type cell wall organization was an enriched term of Th0179 in the *cre1* group.

By investigating the KO functional annotation of the *cre1* and *xyr1* groups, we suggest that both regulators act on the same enzymatic pathways, which was expected due to antagonism in their function, i.e., while CRE1 is the main repressor of genes encoding proteins related to lignocellulose degradation, XYR1 is the main activator of such genes. However, each triggers a specific metabolic pathway according to the strain; therefore, some aspects are noteworthy. For example, it has been reported that the *Trichoderma* species display several mechanisms during their antagonistic action against plant pathogens, including the production of secondary metabolites (Malmierca et al., 2015). According to our findings, due to the highest number of pathways related to secondary metabolites, including the metabolism of terpenoids and polyketides (Mukherjee et al., 2008), we suggest that CRE1 and XYR1 participate in the regulation of secondary metabolism compounds in *T. atroviride*. Furthermore, XYR1 in *T. harzianum* strains appeared to be deeply connected with enzyme pathways related to the metabolism of carbohydrates, especially in the Th3844 strain.

Through a network analysis, we identified transcripts encoding CAZymes coexpressed with *xyr1* and *cre1* in all evaluated strains. We identified CAZyme families responsible for cellulose degradation (e.g., GH12); hemicellulose degradation (e.g., GH16, GH17, CE1, and CE5); pectin degradation (e.g., GH28 and GH93); and other CAZY families with multiple activities or minor activities on lignocellulosic substrates, such as GH2, GH5, GH43, GH95, GH30, and GH39 (de Vries et al., 2017; Kameshwar et al., 2019). Although Ta0020 presented the highest number of GHs coexpressed with CRE1, it was found to be less efficient than the other *Trichoderma* strains in degrading plant biomass (Almeida et al., 2021). In the GH class, enzymes belonging to the GH18 family, which is mainly represented by chitinase-like proteins, are directly related to fungal cell wall degradation in mycoparasite species of *Trichoderma* (Gruber and Seidl-Seiboth 2012). Four GH18 enzymes were coexpressed with CRE1 in *T. atroviride*, which is widely used as a biocontrol agent in agriculture. However, in Ta0020, enzymes from the GH75 family of chitosanases were coexpressed with *xyr1*. Therefore, the degradation of chitosan, which is a partially deacetylated derivative of chitin (Hahn et al., 2020), is a relevant aspect of mycoparasitism that may be influenced by the activity of XYR1. Recently, transcripts encoding GHs were found to be coexpressed with some TFs involved in biomass degradation, e.g., XYR1 (Borin et al., 2018). In the present study, the transcripts encoding hydrolytic enzymes could be sorted into other groups formed in the networks mainly because their expression patterns differed from those of the *xyr1* and *cre1* transcripts.

Several fungal TFs have been described to be directly involved in the regulation of plant biomass utilization (Benocci et al., 2017). Most TFs belong to the zinc cluster family, including Zn<sub>2</sub>Cys<sub>6</sub>- and C<sub>2</sub>H<sub>2</sub>-type TFs, which are characterized by the presence of zinc finger(s) in their binding domains. Most positive regulators appear to belong to the Zn<sub>2</sub>Cys<sub>6</sub> class, while repressors

belong to the C<sub>2</sub>H<sub>2</sub> class (Benocci et al., 2017). Here, we found the highest number of transcripts encoding the Zn<sub>2</sub>Cys<sub>6</sub> and C<sub>2</sub>H<sub>2</sub> classes in the *xyr1* and *cre1* groups of Th0179 and Ta0020, respectively. Both *T. harzianum* strains had a similar profile of transcripts coexpressed with CRE1 and XYR1. However, SteA, a C<sub>2</sub>H<sub>2</sub>-type TF, was coexpressed with the *xyr1* transcript of Th0179. This regulator has been described as an important player in fungal environmental adaptation in response to nutrient deprivation, the production of extracellular proteins involved in the degradation of complex substrates (Hoi and Dumas 2010), and the mediation of the regulatory role of mitogen-activated protein kinase (MAPK) during mycoparasitic responses (Gruber and Zeilinger 2014). In *Aspergillus nidulans*, SteA is required for sexual development (Vallim et al., 2000).

During plant biomass degradation, fungi secrete extracellular enzymes to decompose polysaccharides into small molecules, which are then imported into cells through transporters (Sloothaak et al., 2016). One of the most relevant sugar transporter families in filamentous fungi is the MFS family (Zhang et al., 2013). Here, we found the highest number of transcripts encoding MFS coexpressed with *cre1* and *xyr1* in Ta0020 and Th3844, respectively. Among the *T. harzianum* strains, compared with Th3844, Th0179 showed transcripts encoding several types of transporter proteins, such as transporter proteins of calcium ions (THAR02\_04202, THAR02\_03989, and THAR02\_01350). It has already been reported that metal ions, such as Ca<sup>2+</sup>, have a positive effect on the mycelial growth of *T. reesei* and cellulase production (Chen et al., 2016). This molecular signaling mechanism is mediated by cations transporting ATPase and calcium-dependent mitochondrial carriers, which are both components of Ca<sup>2+</sup>/calmodulin signal transduction, including the TF Crz1 (Chen et al., 2016; Martins-Santana et al., 2020). Therefore, investigating the role of proteins related to calcium transporters in the induction of genes responsive to lignocellulose degradation in Th0179 cells is important since these proteins could transport cations that activate gene expression. Furthermore, transcripts encoding G proteins were coexpressed with *cre1* in Th0179 and Ta0020. Heterotrimeric G proteins have been well studied in several *Trichoderma* species. In saprophytic species, such proteins are involved in the nutrient signaling pathway in connection with a light response, triggering the posttranscriptional regulation of cellulase expression (Hinterdobler et al., 2021); in mycoparasitic species, G protein-coupled receptors are involved in the regulation of processes related to mycoparasitism (Zeilinger and Atanasova 2020).

Although CAZymes, TFs, and transporters play an important role in cellulose degradation, these types of proteins represented only a small percent of the transcripts coexpressed with XYR1 and CRE1 compared to the other protein classes as follows: in the *cre1* group, (I) 10.4% (Th0179), (II) 5.7% (Th3844), and (III) 17.9% (Ta0020), and in the *xyr1* group, (IV) 11.8% (Th0179), (V) 11.9% (Th3844), and (VI) 16% (Ta0020). Since the regulation of genes involved in biomass breakdown is a complex process that involves several signaling pathways, we expected to find proteins with a great range of functions coexpressed with *xyr1* and *cre1*. For example, various kinases and phosphatases were coexpressed with *xyr1* and *cre1* in all

evaluated strains. It has been reported that cellulase gene expression can be regulated by the dynamics of protein phosphorylation and dephosphorylation, which involve protein kinases and phosphatases, respectively (Schmoll et al., 2016). Furthermore, in filamentous fungi, phosphorylation is a prerequisite for CRE1 activity (Cziferszky et al., 2002; Han et al., 2020; de Assis et al., 2021). Therefore, in *T. harzianum*, it is important to elucidate the role of kinases and phosphatases in the regulation of CRE1 function. In all evaluated strains, cytochrome P450 coding genes represented another class of proteins coexpressed in the *cre1* group. It has been reported that these enzymes are important for cells to perform a wide variety of functions, including primary and secondary metabolism, xenobiotic degradation, and cellular defense against plant pathogenic fungi (Siewers et al., 2005; Fan et al., 2013; Chadha et al., 2018). To expand previous findings concerning *Trichoderma* spp. (Chadha et al., 2018), their similar expression pattern with the *cre1* transcript makes them important candidates for an extensive investigation in the cellulose degradation context.

We also investigated the expression profiles of the transcripts in the *cre1* and *xyr1* groups, including *xyr1* and *cre1*, under cellulose and glucose growth. Castro et al. (2016) reported that in *T. reesei*, the expression level of *xyr1* was minimal in the presence of glucose; this phenomenon was not observed in Ta0020 in the present study. In addition, in Ta0020, *cre1* was upregulated in the presence of cellulose, which was not expected due to the role of CRE1 in the repression of cellulolytic and hemicellulolytic enzymes when an easily metabolizable sugar, i.e., glucose, is available in the environment (Benocci et al., 2017). In contrast, in Th3844, the *cre1* expression level in the presence of glucose was higher than that in the presence of cellulose. The gene coexpression networks were modeled based on the transcript expression level under two sets of conditions (cellulose and glucose). Considering that the expression of the *cre1* transcript in Ta0020 was upregulated under cellulose growth, upregulated transcripts were expected and found in the *cre1* group. Recently, Almeida et al. (Almeida et al., 2021) reported that Ta0020 presented the highest number of differentially expressed transcripts under cellulose growth conditions relative to glucose, followed by Th3844 and Th0179. Here, the quantity of upregulated transcripts was low in the *cre1* and *xyr1* groups of the *T. harzianum* strains. These results may indicate that both TFs have a basal expression level at 96 h of fermentation; thus, the transcripts grouped with such regulatory proteins presented the same expression pattern and, mostly, were not differentially expressed transcripts.

## 4.2 Examining the Network's Topology

To extract additional information from the networks, we characterized the network topologies of the modules identified separately. We might infer that many transcripts were under the influence of the repressor CRE1 in Ta0020, while in the *T. harzianum* strains, the transcripts seem to have been affected by the activator XYR1. Therefore, the described profiles may indicate that in *T. harzianum*, the transcripts, including those encoding

XYR1, act together to perform a determined biological function that is favorable to the expression of genes related to cellulose degradation. In contrast, in *T. atroviride*, the transcripts in the *cre1* group appeared to act on the same biological process, which may be related to the repression of genes encoding hydrolytic enzymes and other proteins required for cellulose degradation.

Hub transcripts were identified in the *cre1* and *xyr1* groups, and new targets were discovered. In the *cre1* group, a transcript with a SET-domain coding gene was found as a hub node of Th3844. Such SET-domain proteins participate in chromatin modifications by methylating specific lysines on the histone tails (Kouzarides 2007). In filamentous fungi, the epigenetic regulation of holocellulase gene expression has already been reported (Zeilinger et al., 2003), and CRE1 plays an important role in nucleosome positioning (Ries et al., 2014). Interestingly, ATP synthase, which synthesizes ATP from ADP and inorganic phosphate on mitochondria (Burger et al., 2003), was found to be a hub node of Th0179. Thus, we might infer that a great number of transcripts were coexpressed with a hub node related to mitochondrial ATP production, which is the main energy source for intracellular metabolic pathways (Neupane et al., 2019). In the *xyr1* group, a transcript encoding an ATP-dependent RNA helicase was found as a hub node of Th3844. Such enzymes catalyze the ATP-dependent separation of double-stranded RNA and participate in nearly all aspects of RNA metabolism (Jankowsky 2011). Additionally, the *sepA* transcript was identified as a hub node of Th0179. In *Aspergillus nidulans*, the *sepA* gene encodes a member of the FH1/2 protein family, which is involved in cytokinesis and the maintenance of cellular polarity, i.e., related to the cell division process (Harris et al., 1997). Overall, our findings suggest that the hub genes were not necessarily the most effective genes related to lignocellulose deconstruction, confirming the indirect action of XYR1 and CRE1 in *T. harzianum* on regulatory hydrolysis mechanisms. In Ta0020, transcripts encoding hypothetical proteins were identified as potential hub nodes in both groups, providing new targets for further studies evaluating their functions in fungal physiology.

We also investigated the first neighbors of the *cre1* and *xyr1* transcripts in the modeled global HRR networks of all evaluated strains. While Ta0020 showed differentially expressed transcripts as the first neighbor of the *cre1* transcript, interestingly, both *T. harzianum* strains presented the opposite profile in which only the first neighbors of the *xyr1* transcript were differentially expressed. In addition, the evaluated strains showed different numbers of neighbors of the *cre1* and *xyr1* transcripts, which were distributed among several groups. Such a divergent profile may indicate that each TF affects a set of transcripts in a specific way that varies among the strains. Overall, we identified CAZymes, TFs, and transporters as first neighbors of *cre1* and *xyr1*, confirming the results obtained in this study using the WGCNA approach.

Another property of a network's topology is the shortest paths connecting two transcripts (Pavlopoulos et al., 2011). Here, the significant shortest paths between both studied TFs, i.e., CRE1 and XYR1, and the CAZymes with a higher-level expression under cellulose growth conditions were investigated in all strains. The average shortest pathway distance between the transcripts

encoding CRE1 or XYR1 and all selected CAZymes was relatively short, which may be attributed to a network phenomenon called the small-world effect, i.e., networks can be highly clustered with a small number of necessary steps to reach one node from another (Maier 2019). However, several aspects should be highlighted. We identified CAZymes responsible for cellulose degradation, such as GH6 (Th0179 and Ta0020), and other CAZy families with multiple activities or minor activities on lignocellulosic substrates, such as GH1 and GH5 (Th0179) (de Vries et al., 2017; Kameshwar et al., 2019) with a low number of minimum pathways to CRE1 in Ta0020. In contrast, CAZymes responsible for cellulose degradation, such as CBM1 domain (Th3844 and Ta0020) and GH7 (Ta0020), for hemicellulose degradation, such as GH55 (Th0179), and CAZy families with multiple activities or minor activities on lignocellulosic substrates, such as GH3 (Th3844) and GH1 (Ta0020) (de Vries et al., 2017; Kameshwar et al., 2019), were identified with a high number of minimum pathways to XYR1. Because certain shortest paths are not necessarily unique, we also considered the number of possibilities that the paths may occur. Our results suggest that the number of possible minimum paths between some CAZymes and CRE1 or XYR1 was higher than of others. For example, a great number of possible shortest paths was observed between CRE1 and GH6 in Ta0020 and between CRE1 and GH10, GH6, or GH1 in Th0179. In contrast, in Ta0020, such profiles were observed between XYR1 and CAZymes with cellulolytic (AA9) and hemicellulolytic activities (GH16) and between CRE1 and GH6 with a CBM1 domain.

Furthermore, we performed a shortest path analysis to explore transitive transcripts between two nodes. Considering that the lowest number of transitive transcripts between two nodes may indicate the need for fewer signal pathways, representing a more direct relation, we chose to investigate the shortest paths with only one transcript between the desired targets. Interestingly, transcripts encoding proteins related to ATP synthesis were found between GH45 with a CBM1 domain and *cre1* and between GH1 and *cre1* in Th3844, which could be explained by the demand for energy required for CRE1 to exercise its repressor activity on these hydrolytic enzymes. However, in Th3844, a transcript encoding a protein involved in quality control processes that center on the endoplasmic reticulum was found between GH16 and *cre1*, indicating that a signaling pathway is triggered by CRE1 to repress the expression of such an enzyme. Curiously, in Ta0020, a phosphotyrosine phosphatase was found in the shortest path between GH1, which is a homolog of GH1 in the *T. harzianum* strains, and *cre1*. Such proteins are involved in posttranslational modification, including the phosphorylation process, which plays an essential role in signal transduction to achieve CCR by CRE1 (Horta et al., 2019; Han et al., 2020). In Th3844, we found a transcript encoding a protein related to the transport of substances across the mitochondrial membrane between CBM1 and *xyr1*, which may indicate high cellular activity and, therefore, a high demand for energy for gene expression. In Ta0020, a transcript encoding a protein involved in the regulation of chromatin and gene expression was found between GH1 and *xyr1*, which may indicate an intermediated process for the expression of such an enzyme.

In conclusion, biological networks represent a powerful approach to accelerate the elucidation of the molecular mechanisms underlying important biological processes. Our findings suggest that the set of transcripts related to XYR1 and CRE1 varies among the studied *T. harzianum* strains, suggesting regulatory differences in enzymatic hydrolysis. These findings corroborate previous studies in which differences in biomass degradation and enzyme production between strains of the same species have been reported (de Vries et al., 2017; Thanh et al., 2019; Tolgo et al., 2021). Furthermore, such transcripts were not limited to CAZymes and other proteins related to biomass degradation. Thus, we suggest that both TFs play a role in the undirected regulation of gene encoding proteins related to cellulose degradation, and multiple pathways related to gene regulation, protein expression, and posttranslational modifications may be triggered by the studied TFs. We expect that our results could contribute to a better understanding of fungal biodiversity, especially regarding the transcription regulation involved in hydrolytic enzyme expression in *T. harzianum*. By describing new potential targets involved in the cellulose degradation pathway, this knowledge can be used to develop genetic manipulation strategies and expand the use of *T. harzianum* as an enzyme producer in biotechnological industrial applications.

## DATA AVAILABILITY STATEMENT

The original contributions presented in the study are included in the article/**Supplementary Material**, further inquiries can be directed to the corresponding author.

## AUTHOR CONTRIBUTIONS

RR: Writing—original draft, Methodology, and Conceptualization. AA: Methodology, Software, Writing—review and editing, and Formal analysis. DA: Resources, and Writing—review and editing. JF: Writing—review and editing. MH: Resources and Writing—review and editing. AS: Supervision, review and editing, and funding acquisition.

## FUNDING

Financial support for this work was provided by the São Paulo Research Foundation (FAPESP) (Process number 2015/09202-0 and 2018/19660-4), the Coordination of Improvement of Higher Education Personnel (CAPES, Computational Biology Program, Process number 88882.160095/2013-01) and the Brazilian National Council for Technological and Scientific Development (CNPq, Process number 312777/2018-3). RR received a master's fellowship from CAPES (88887.176241/2018-00 and 88882.329483/2019-01) and a PhD fellowship from CAPES (88887.482201/2020-00) and FAPESP (2020/13420-1). AA received a PhD fellowship from FAPESP (2019/03232-6). AS received a research fellowship from CNPq (312777/2018-3).

## ACKNOWLEDGMENTS

We are grateful to the Brazilian Biorenewables National Laboratory (LNBR), Campinas—SP for conducting the fermentation experiments; the Center of Molecular Biology and Genetic Engineering (CBMEG) at the University of Campinas, SP for the use of the center and laboratory space; and the São Paulo Research Foundation (FAPESP), the Coordination of Improvement of Higher Education Personnel (CAPES, Computational Biology Program), and

the Brazilian National Council for Technological and Scientific Development (CNPq) for supporting the project and researchers.

## SUPPLEMENTARY MATERIAL

The Supplementary Material for this article can be found online at: <https://www.frontiersin.org/articles/10.3389/fgene.2022.807243/full#supplementary-material>

## REFERENCES

- Adnan, M., Zheng, W., Islam, W., Arif, M., Abubakar, Y., Wang, Z., et al. (2017). Carbon Catabolite Repression in Filamentous Fungi. *Ijms* 19, 48. doi:10.3390/ijms19010048
- Alazi, E., and Ram, A. F. J. (2018). Modulating Transcriptional Regulation of Plant Biomass Degrading Enzyme Networks for Rational Design of Industrial Fungal Strains. *Front. Bioeng. Biotechnol.* 6, 133. doi:10.3389/fbioe.2018.00133
- Alexa, A., and Rahnenfuhrer, J. (2021). topGO: Enrichment Analysis for Gene Ontology. R Package Version 2.44.0.
- Almeida, D. A., Horta, M. A. C., Ferreira Filho, J. A., Murad, N. F., and de Souza, A. P. (2021). The Synergistic Actions of Hydrolytic Genes Reveal the Mechanism of *Trichoderma harzianum* for Cellulose Degradation. *J. Biotechnol.* 334, 1–10. doi:10.1016/j.jbiotec.2021.05.001
- Antoniêto, A. C. C., dos Santos Castro, L., Silva-Rocha, R., Persinoti, G. F., and Silva, R. N. (2014). Defining the Genome-wide Role of CRE1 during Carbon Catabolite Repression in *Trichoderma reesei* Using RNA-Seq Analysis. *Fungal Genet. Biol.* 73, 93–103. doi:10.1016/j.fgb.2014.10.009
- Arntzen, M. Ø., Bengtsson, O., Várnai, A., Delogu, F., Mathiesen, G., and Eijssink, V. G. H. (2020). Quantitative Comparison of the Biomass-Degrading Enzyme Repertoires of Five Filamentous Fungi. *Sci. Rep.* 10, 20267. doi:10.1038/s41598-020-75217-z
- Ashburner, M., Ball, C. A., Blake, J. A., Botstein, D., Butler, H., Cherry, J. M., et al. (2000). Gene Ontology: Tool for the Unification of Biology. *Nat. Genet.* 25, 25–29. doi:10.1038/75556
- Baroncelli, R., Piaggieschi, G., Fiorini, L., Bertolini, E., Zapparata, A., Pè, M. E., et al. (2015). Draft Whole-Genome Sequence of the Biocontrol Agent *Trichoderma harzianum* T6776. *Genome Announc* 3, e00647–15. doi:10.1128/genomeA.00647-15
- Benocci, T., Aguilar-Pontes, M. V., Zhou, M., Seiboth, B., and de Vries, R. P. (2017). Regulators of Plant Biomass Degradation in Ascomycetous Fungi. *Biotechnol. Biofuels* 10, 152. doi:10.1186/s13068-017-0841-x
- Bischof, R. H., Ramoni, J., and Seiboth, B. (2016). Cellulases and beyond: the First 70 Years of the Enzyme Producer *Trichoderma reesei*. *Microb. Cel Fact.* 15, 106. doi:10.1186/s12934-016-0507-6
- Borin, G. P., Carazzolle, M. F., Dos Santos, R. A. C., Riaño-Pachón, D. M., and Oliveira, J. V. d. C. (2018). Gene Co-expression Network Reveals Potential New Genes Related to Sugarcane Bagasse Degradation in *Trichoderma reesei* RUT-30. *Front. Bioeng. Biotechnol.* 6, 151. doi:10.3389/fbioe.2018.00151
- Burger, G., Gray, M. W., and Franz Lang, B. (2003). Mitochondrial Genomes: Anything Goes. *Trends Genet.* 19, 709–716. doi:10.1016/j.tig.2003.10.012
- Chadha, S., Mehrete, S. T., Bansal, R., Kuo, A., Aerts, A., Grigoriev, I. V., et al. (2018). Genome-wide Analysis of Cytochrome P450s of *Trichoderma* spp. Annotation and Evolutionary Relationships. *Fungal Biol. Biotechnol.* 5, 12. doi:10.1186/s40694-018-0056-3
- Chen, L., Zou, G., Wang, J., Wang, J., Liu, R., Jiang, Y., et al. (2016). Characterization of the Ca<sup>2+</sup>-Responsive Signaling Pathway in Regulating the Expression and Secretion of Cellulases in *Trichoderma reesei* Rut-C30. *Mol. Microbiol.* 100, 560–575. doi:10.1111/mmi.13334
- Cock, P. J. A., Antao, T., Chang, J. T., Chapman, B. A., Cox, C. J., Dalke, A., et al. (2009). Biopython: Freely Available Python Tools for Computational Molecular Biology and Bioinformatics. *Bioinformatics* 25, 1422–1423. doi:10.1093/bioinformatics/btp163
- Cortijo, S., Bhattarai, M., Locke, J. C. W., and Ahnert, S. E. (2020). Co-expression Networks from Gene Expression Variability between Genetically Identical Seedlings Can Reveal Novel Regulatory Relationships. *Front. Plant Sci.* 11. doi:10.3389/fpls.2020.599464
- Cziferszky, A., Mach, R. L., and Kubicek, C. P. (2002). Phosphorylation Positively Regulates DNA Binding of the Carbon Catabolite Repressor CreI of *Hypocrea jecorina* (*Trichoderma reesei*). *J. Biol. Chem.* 277, 14688–14694. doi:10.1074/jbc.M200744200
- da Silva Delabona, P., Rodrigues, G. N., Zubieta, M. P., Ramoni, J., Codima, C. A., Lima, D. J., et al. (2017). The Relation between Xyr1 Overexpression in *Trichoderma harzianum* and Sugarcane Bagasse Saccharification Performance. *J. Biotechnol.* 246, 24–32. doi:10.1016/j.jbiotec.2017.02.002
- de Assis, L. J., Ries, L. N. A., Savoldi, M., Dos Reis, T. F., Brown, N. A., and Goldman, G. H. (2015). *Aspergillus nidulans* Protein Kinase A Plays an Important Role in Cellulase Production. *Biotechnol. Biofuels* 8, 213. doi:10.1186/s13068-015-0401-1
- de Assis, L. J., Silva, L. P., Bayram, O., Dowling, P., Kniemeyer, O., Krüger, T., et al. (2021). Carbon Catabolite Repression in Filamentous Fungi Is Regulated by Phosphorylation of the Transcription Factor CreA. *mBio* 12, e03146–20. doi:10.1128/mBio.03146-20
- de Vries, R. P., Riley, R., Wiebenga, A., Aguilar-Osorio, G., Amillis, S., Uchima, C. A., et al. (2017). Comparative Genomics Reveals High Biological Diversity and Specific Adaptations in the Industrially and Medically Important Fungal Genus *Aspergillus*. *Genome Biol.* 18, 28. doi:10.1186/s13059-017-1151-0
- Delabona, P. d. S., Codima, C. A., Ramoni, J., Zubieta, M. P., de Araújo, B. M., Farinas, C. S., et al. (2020). The Impact of Putative Methyltransferase Overexpression on the *Trichoderma harzianum* Cellulolytic System for Biomass Conversion. *Bioresour. Techn.* 313, 123616. doi:10.1016/j.biortech.2020.123616
- Delabona, P. d. S., Lima, D. J., Codima, C. A., Ramoni, J., Gelain, L., de Melo, V. S., et al. (2021). Replacement of the Carbon Catabolite Regulator (Cre1) and Fed-Batch Cultivation as Strategies to Enhance Cellulase Production in *Trichoderma harzianum*. *Bioresour. Techn. Rep.* 13, 100634. doi:10.1016/j.biteb.2021.100634
- Dodd, S. L., Lieckfeldt, E., and Samuels, G. J. (2003). *Hypocrea Atroviridis* Sp. nov., the Teleomorph of *Trichoderma Atroviride*. *Mycologia* 95, 27–40. doi:10.1080/15572536.2004.11833129
- dos Santos Castro, L., de Paula, R. G., Antoniêto, A. C. C., Persinoti, G. F., Silva-Rocha, R., and Silva, R. N. (2016). Understanding the Role of the Master Regulator XYR1 in *Trichoderma reesei* by Global Transcriptional Analysis. *Front. Microbiol.* 7, 175. doi:10.3389/fmicb.2016.00175
- Druzhinina, I. S., Chenthamara, K., Zhang, J., Atanasova, L., Yang, D., Miao, Y., et al. (2018). Massive Lateral Transfer of Genes Encoding Plant Cell wall-degrading Enzymes to the Mycoparasitic Fungus *Trichoderma* from its Plant-Associated Hosts. *Plos Genet.* 14, e1007322. doi:10.1371/journal.pgen.1007322
- Druzhinina, I. S., Kopchinskiy, A. G., and Kubicek, C. P. (2006). The First 100 *Trichoderma* Species Characterized by Molecular Data. *Mycoscience* 47, 55–64. doi:10.1007/s10267-006-0279-7
- Druzhinina, I. S., Kubicek, C. P., Komon-Zelazowska, M., Belayneh Mulaw, T., and Bissett, J. (2010). The *Trichoderma harzianum* Demon: Complex Speciation History Resulting in Coexistence of Hypothetical Biological Species, Recent Agamospecies and Numerous Relict Lineages. *BMC Evol. Biol.* 10, 94. doi:10.1186/1471-2148-10-94
- Fan, J., Urban, M., Parker, J. E., Brewer, H. C., Kelly, S. L., Hammond-Kosack, K. E., et al. (2013). Characterization of the Sterol 14 $\alpha$ -demethylases of *Fusarium*



- Graminearum Identifies a Novel Genus-specific CYP 51 Function. *New Phytol.* 198, 821–835. doi:10.1111/nph.12193
- Felsenstein, J. (1985). Confidence Limits on Phylogenies: an Approach Using the Bootstrap. *Evolution* 39, 783–791. doi:10.2307/240867810.1111/j.1558-5646.1985.tb00420.x
- Fonseca, L. M., Parreiras, L. S., and Murakami, M. T. (2020). Rational Engineering of the *Trichoderma Reesei* RUT-C30 Strain into an Industrially Relevant Platform for Cellulase Production. *Biotechnol. Biofuels* 13 (1), 93. doi:10.1186/s13068-020-01732-w
- Grevel, A., and Becker, T. (2020). Porins as Helpers in Mitochondrial Protein Translocation. *Biol. Chem.* 401, 699–708. doi:10.1515/hsz-2019-0438
- Gruber, S., and Seidl-Seiboth, V. (2012). Self versus Non-self: Fungal Cell wall Degradation in *Trichoderma*. *Microbiology (Reading)* 158, 26–34. doi:10.1099/mic.0.052613-0
- Gruber, S., and Zeilinger, S. (2014). The Transcription Factor Ste12 Mediates the Regulatory Role of the Tmk1 MAP Kinase in Mycoparasitism and Vegetative Hyphal Fusion in the Filamentous Fungus *Trichoderma Atroviride*. *PLoS One* 9, e111636. doi:10.1371/journal.pone.0111636
- Hahn, T., Tafi, E., Paul, A., Salvia, R., Falabella, P., and Zibek, S. (2020). Current State of Chitin Purification and Chitosan Production from Insects. *J. Chem. Technol. Biotechnol.* 95, 2775–2795. doi:10.1002/jctb.6533
- Han, L., Tan, Y., Ma, W., Niu, K., Hou, S., Guo, W., et al. (2020). Precision Engineering of the Transcription Factor Cre1 in *Hypocrea Jecorina* (*Trichoderma Reesei*) for Efficient Cellulase Production in the Presence of Glucose. *Front. Bioeng. Biotechnol.* 8, 852. doi:10.3389/fbioe.2020.00852
- Harris, S. D., Hamer, L., Sharpless, K. E., and Hamer, J. E. (1997). The *Aspergillus nidulans* sepA Gene Encodes an FH1/2 Protein Involved in Cytokinesis and the Maintenance of Cellular Polarity. *EMBO J.* 16, 3474–3483. doi:10.1093/emboj/16.12.3474
- Hinterdobler, W., Li, G., Turrà, D., Schalamun, M., Kindel, S., Sauer, U., et al. (2021). Integration of Chemosensing and Carbon Catabolite Repression Impacts Fungal Enzyme Regulation and Plant Associations. *bioRxiv*. 2021.05.06.442915.
- Horta, M. A. C., Filho, J. A. F., Murad, N. F., de Oliveira Santos, E., Dos Santos, C. A., Mendes, J. S., et al. (2018). Network of Proteins, Enzymes and Genes Linked to Biomass Degradation Shared by *Trichoderma* Species. *Sci. Rep.* 8, 1341. doi:10.1038/s41598-018-19671-w
- Horta, M. A. C., Thieme, N., Gao, Y., Burnum-Johnson, K. E., Nicora, C. D., Gritsenko, M. A., et al. (2019). Broad Substrate-specific Phosphorylation Events Are Associated with the Initial Stage of Plant Cell Wall Recognition in *Neurospora Crassa*. *Front. Microbiol.* 10, 2317. doi:10.3389/fmicb.2019.02317
- Jankowsky, E. (2011). RNA Helicases at Work: Binding and Rearranging. *Trends Biochem. Sci.* 36, 19–29. doi:10.1016/j.tibs.2010.07.008
- Jones, D. T., Taylor, W. R., and Thornton, J. M. (1992). The Rapid Generation of Mutation Data Matrices from Protein Sequences. *Bioinformatics* 8, 275–282. doi:10.1093/bioinformatics/8.3.275
- Kameshwar, A. K. S., Ramos, L. P., and Qin, W. (2019). CAZymes-Based Ranking of Fungi (CBRF): an Interactive Web Database for Identifying Fungi with Extrinsic Plant Biomass Degrading Abilities. *Bioresour. Bioproc.* 6, 51. doi:10.1186/s40643-019-0286-0
- Kanehisa, M., and Goto, S. (2000). KEGG: Kyoto Encyclopedia of Genes and Genomes. *Nucleic Acids Res.* 28, 27–30. doi:10.1093/nar/28.1.27
- Kimura, M. (1980). A Simple Method for Estimating Evolutionary Rates of Base Substitutions through Comparative Studies of Nucleotide Sequences. *J. Mol. Evol.* 16, 111–120. doi:10.1007/BF01731581
- Klaubauf, S., Narang, H. M., Post, H., Zhou, M., Brunner, K., Mach-Aigner, A. R., et al. (2014). Similar Is Not the Same: Differences in the Function of the (Hemi-) cellulolytic Regulator XlnR (Xlr1/Xyr1) in Filamentous Fungi. *Fungal Genet. Biol.* 72, 73–81. doi:10.1016/j.fgb.2014.07.007
- Kolde, R. (2019). Pheatmap: Pretty Heatmaps. R Package Version 1.0.12.
- Koutrouli, M., Karatzas, E., Paez-Espino, D., and Pavlopoulos, G. A. (2020). A Guide to Conquer the Biological Network Era Using Graph Theory. *Front. Bioeng. Biotechnol.* 8, 34. doi:10.3389/fbioe.2020.00034
- Kouzarides, T. (2007). Chromatin Modifications and Their Function. *Cell* 128, 693–705. doi:10.1016/j.cell.2007.02.005
- Kubicek, C. P., Herrera-Estrella, A., Seidl-Seiboth, V., Martinez, D. A., Druzhinina, I. S., Thon, M., et al. (2011). Comparative Genome Sequence Analysis Underscores Mycoparasitism as the Ancestral Life Style of *Trichoderma*. *Genome Biol.* 12, R40. doi:10.1186/gb-2011-12-4-r40
- Kubicek, C. P., Steindorff, A. S., Chenthamara, K., Manganiello, G., Henrissat, B., Zhang, J., et al. (2019). Evolution and Comparative Genomics of the Most Common *Trichoderma* Species. *BMC Genomics* 20, 485. doi:10.1186/s12864-019-5680-7
- Kumar, S., Stecher, G., and Tamura, K. (2016). MEGA7: Molecular Evolutionary Genetics Analysis Version 7.0 for Bigger Datasets. *Mol. Biol. Evol.* 33, 1870–1874. doi:10.1093/molbev/msw054
- Langfelder, P., and Horvath, S. (2008). WGCNA: an R Package for Weighted Correlation Network Analysis. *BMC Bioinformatics* 9, 559. doi:10.1186/1471-2105-9-559
- Langfelder, P., Zhang, B., and Horvath, S. (2008). Defining Clusters from a Hierarchical Cluster Tree: the Dynamic Tree Cut Package for R. *Bioinformatics* 24, 719–720. doi:10.1093/bioinformatics/btm563
- Li, C.-X., Zhao, S., Luo, X.-M., and Feng, J.-X. (2020). Weighted Gene Co-expression Network Analysis Identifies Critical Genes for the Production of Cellulase and Xylanase in *Penicillium Oxalicum*. *Front. Microbiol.* 11, 520. doi:10.3389/fmicb.2020.00520
- Li, J.-X., Zhang, F., Jiang, D.-D., Li, J., Wang, F.-L., Zhang, Z., et al. (2020). Diversity of Cellulase-Producing Filamentous Fungi from Tibet and Transcriptomic Analysis of a superior Cellulase Producer *Trichoderma harzianum* LZ117. *Front. Microbiol.* 11, 1617. doi:10.3389/fmicb.2020.01617
- Lichius, A., Seidl-Seiboth, V., Seiboth, B., and Kubicek, C. P. (2014). Nucleocytoplasmic Shuttling Dynamics of the Transcriptional regulators XYR1 and CRE1 under Conditions of Cellulase and Xylanase Gene Expression in *Trichoderma Reesei*. *Mol. Microbiol.* 94, 1162–1178. doi:10.1111/mmi.12824
- Liu, J., Liu, S., and Yang, X. (2021). Construction of Gene Modules and Analysis of Prognostic Biomarkers for Cervical Cancer by Weighted Gene Co-expression Network Analysis. *Front. Oncol.* 11. doi:10.3389/fonc.2021.542063
- Liu, R., Chen, L., Jiang, Y., Zou, G., and Zhou, Z. (2017). A Novel Transcription Factor Specifically Regulates GH11 Xylanase Genes in *Trichoderma Reesei*. *Biotechnol. Biofuels* 10 (1), 194. doi:10.1186/s13068-017-0878-x
- Lombard, V., Golaconda Ramulu, H., Drula, E., Coutinho, P. M., and Henrissat, B. (2014). The Carbohydrate-Active Enzymes Database (CAZy) in 2013. *Nucl. Acids Res.* 42, D490–D495. doi:10.1093/nar/gkt1178
- Luscombe, N. M., Babu, M. M., Yu, H., Snyder, M., Teichmann, S. A., and Gerstein, M. (2004). Genomic Analysis of Regulatory Network Dynamics Reveals Large Topological Changes. *Nature* 431, 308–312. doi:10.1038/nature02782
- Mach-Aigner, A. R., Pucher, M. E., Steiger, M. G., Bauer, G. E., Preis, S. J., and Mach, R. L. (2008). Transcriptional Regulation of Xyr1, Encoding the Main Regulator of the Xylanolytic and Cellulolytic Enzyme System in *Hypocrea Jecorina*. *Appl. Environ. Microbiol.* 74, 6554–6562. doi:10.1128/AEM.01143-08
- Maier, B. F. (2019). Generalization of the Small-World Effect on a Model Approaching the Erdős-Rényi Random Graph. *Sci. Rep.* 9, 9268. doi:10.1038/s41598-019-45576-3
- Malmierca, M. G., McCormick, S. P., Cardoza, R. E., Alexander, N. J., Monte, E., and Gutiérrez, S. (2015). Production of Trichodiene by *Trichoderma Harzianum* Alters the Perception of This Biocontrol Strain by Plants and Antagonized Fungi. *Environ. Microbiol.* 17, 2628–2646. doi:10.1111/1462-2920.12506
- Martinez, D., Berka, R. M., Henrissat, B., Saloheimo, M., Arvas, M., Baker, S. E., et al. (2008). Genome Sequencing and Analysis of the Biomass-Degrading Fungus *Trichoderma Reesei* (Syn. *Hypocrea Jecorina*). *Nat. Biotechnol.* 26, 553–560. doi:10.1038/nbt1403
- Martins-Santana, L., Paula, R. G. d., Silva, A. G., Lopes, D. C. B., Silva, R. d. N., and Silva-Rocha, R. (2020). CRZ1 Regulator and Calcium Cooperatively Modulate Holocellulases Gene Expression in *Trichoderma Reesei* QM6a. *Genet. Mol. Biol.* 43, e20190244. doi:10.1590/1678-4685-GMB-2019-0244
- Maruyama, C. R., Bilesky-José, N., de Lima, R., and Fraceto, L. F. (2020). Encapsulation of *Trichoderma harzianum* Preserves Enzymatic Activity and Enhances the Potential for Biological Control. *Front. Bioeng. Biotechnol.* 8, 225. doi:10.3389/fbioe.2020.00225
- Medeiros, H. A. d., Araújo Filho, J. V. d., Freitas, L. G. d., Castillo, P., Rubio, M. B., Hermosa, R., et al. (2017). Tomato Progeny Inherits Resistance to the Nematode *Meloidogyne javanica* Linked to Plant Growth Induced by the Biocontrol Fungus *Trichoderma Atroviride*. *Sci. Rep.* 7, 40216. doi:10.1038/srep40216

- Mello-de-Sousa, T. M., Gorsche, R., Rassinger, A., Poças-Fonseca, M. J., Mach, R. L., and Mach-Aigner, A. R. (2014). A Truncated Form of the Carbon Catabolite Repressor 1 Increases Cellulase Production in *Trichoderma Reesei*. *Biotechnol. Biofuels* 7, 129. doi:10.1186/s13068-014-0129-3
- Monroy, A. A., Stappler, E., Schuster, A., Sulyok, M., and Scholl, M. (2017). A CRE1- Regulated Cluster Is Responsible for Light Dependent Production of Dihydrotrichotetronin in *Trichoderma Reesei*. *PLoS One* 12, e0182530. doi:10.1371/journal.pone.0182530
- Mukherjee, P. K., Nautiyal, C. S., and Mukhopadhyay, A. N. (2008). "Molecular Mechanisms of Biocontrol by *Trichoderma* Spp.," in *Molecular Mechanisms of Plant and Microbe Coexistence*. Editors C. S. Nautiyal and P. Dion (Berlin, Heidelberg: Springer), 243–262. doi:10.1007/978-3-540-75575-3\_10
- Mutwil, M., Usadel, B. r., Schuette, M., Loraine, A., Ebenhoeh, O., and Persson, S. (2009). Assembly of an Interactive Correlation Network for the Arabidopsis Genome Using a Novel Heuristic Clustering Algorithm. *Plant Physiol.* 152, 29–43. doi:10.1104/pp.109.145318
- Nasa, I., and Kettenbach, A. N. (2018). Coordination of Protein Kinase and Phosphoprotein Phosphatase Activities in Mitosis. *Front. Cel Dev. Biol.* 6, 30. doi:10.3389/fcell.2018.00030
- Neupane, P., Bhujii, S., Thapa, N., and Bhattarai, H. K. (2019). ATP Synthase: Structure, Function and Inhibition. *Biomol. Concepts* 10, 1–10. doi:10.1515/bmc-2019-0001
- Pavlopoulos, G. A., Secrier, M., Moschopoulos, C. N., Soldatos, T. G., Kossida, S., Aerts, J., et al. (2011). Using Graph Theory to Analyze Biological Networks. *BioData Mining* 4, 10. doi:10.1186/1756-0381-4-10
- Phillips, B. P., Gomez-Navarro, N., and Miller, E. A. (2020). Protein Quality Control in the Endoplasmic Reticulum. *Curr. Opin. Cel Biol.* 65, 96–102. doi:10.1016/j.ccb.2020.04.002
- Portnoy, T., Margeot, A., Linke, R., Atanasova, L., Fekete, E., Sándor, E., et al. (2011). The CRE1 Carbon Catabolite Repressor of the Fungus *Trichoderma Reesei*: a Master Regulator of Carbon Assimilation. *BMC Genomics* 12, 269. doi:10.1186/1471-2164-12-269
- R Core Team (2018). *R: A Language and Environment for Statistical Computing*. Vienna, Austria: R Foundation for Statistical Computing.
- Reithner, B., Mach-Aigner, A. R., Herrera-Estrella, A., and Mach, R. L. (2014). *Trichoderma Atroviride* Transcriptional Regulator Xyr1 Supports the Induction of Systemic Resistance in Plants. *Appl. Environ. Microbiol.* 80, 5274–5281. doi:10.1128/AEM.00930-14
- Ries, L., Belshaw, N. J., Ilmén, M., Penttilä, M. E., Alapuranen, M., and Archer, D. B. (2014). The Role of CRE1 in Nucleosome Positioning within the Cbh1 Promoter and Coding Regions of *Trichoderma Reesei*. *Appl. Microbiol. Biotechnol.* 98, 749–762. doi:10.1007/s00253-013-5354-3
- Sanner, M. F. (1999). Python: a Programming Language for Software Integration and Development. *J. Mol. Graph. Model.* 17, 57–61. doi:10.1186/1471-2105-4-2
- Saravankumar, K., Li, Y., Yu, C., Wang, Q.-q., Wang, M., Sun, J., et al. (2017). Effect of *Trichoderma harzianum* on maize Rhizosphere Microbiome and Biocontrol of Fusarium Stalk Rot. *Sci. Rep.* 7, 1771. doi:10.1038/s41598-017-01680-w
- Scardoni, G., Tosadori, G., Pratap, S., Spoto, F., and Laudanna, C. (2016). Finding the Shortest Path with PesCa: a Tool for Network Reconstruction. *F1000Res* 4, 484. doi:10.12688/f1000research.6769.2
- Schmoll, M., Dattenböck, C., Carreras-Villaseñor, N., Mendoza-Mendoza, A., Tisch, D., Alemán, M. I., et al. (2016). The Genomes of Three Uneven Siblings: Footprints of the Lifestyles of Three *Trichoderma* Species. *Microbiol. Mol. Biol. Rev.* 80, 205–327. doi:10.1128/MMBR.00040-15
- Schmoll, M. (2018). Light, Stress, Sex and Carbon - the Photoreceptor ENVOY as a central Checkpoint in the Physiology of *Trichoderma Reesei*. *Fungal Biol.* 122, 479–486. doi:10.1016/j.funbio.2017.10.007
- Schoch, C. L., Seifert, K. A., Huhndorf, S., Robert, V., Spouge, J. L., Levesque, C. A., et al. (2012). Nuclear Ribosomal Internal Transcribed Spacer (ITS) Region as a Universal DNA Barcode Marker for Fungi. *Proc. Natl. Acad. Sci. U. S. A.* 109, 6241–6246. doi:10.1073/pnas.1117018109
- Shannon, P., Markiel, A., Ozier, O., Baliga, N. S., Wang, J. T., Ramage, D., et al. (2003). Cytoscape: a Software Environment for Integrated Models of Biomolecular Interaction Networks. *Genome Res.* 13, 2498–2504. doi:10.1101/gr.1239303
- Siewers, V., Viaud, M., Jimenez-Teja, D., Collado, I. G., Gronover, C. S., Pradier, J.-M., et al. (2005). Functional Analysis of the Cytochrome P450 Monooxygenase Gene Bcbot1 of *Botrytis Cinerea* Indicates that Botrydial Is a Strain-specific Virulence Factor. *Mpmi* 18, 602–612. doi:10.1094/MPMI-18-0602
- Sloothaak, J., Tamayo-Ramos, J. A., Odoni, D. I., Laothanachareon, T., Derntl, C., Mach-Aigner, A. R., et al. (2016). Identification and Functional Characterization of Novel Xylose Transporters from the Cell Factories *Aspergillus niger* and *Trichoderma Reesei*. *Biotechnol. Biofuels* 9, 148. doi:10.1186/s13068-016-0564-4
- Strauss, J., Mach, R. L., Zeilinger, S., Hartler, G., Stöffler, G., Wolschek, M., et al. (1995). Cre1, the Carbon Catabolite Repressor Protein from *Trichoderma Reesei*. *FEBS Lett.* 376, 103–107. doi:10.1016/0014-5793(95)01255-5
- Stricker, A. R., Grosstessner-Hain, K., Würlleitner, E., and Mach, R. L. (2006). Xyr1 (Xylanase Regulator 1) Regulates Both the Hydrolytic Enzyme System and D-Xylose Metabolism in *Hypocrea Jecorina*. *Eukaryot. Cel* 5, 2128–2137. doi:10.1128/EC.00211-06
- Supek, F., Bošnjak, M., Škunca, N., and Šmuc, T. (2011). REVIGO Summarizes and Visualizes Long Lists of Gene Ontology Terms. *PLoS One* 6, e21800. doi:10.1371/journal.pone.0021800
- Thanh, V. N., Thuy, N. T., Huong, H. T. T., Hien, D. D., Hang, D. T. M., Anh, D. T. K., et al. (2019). Surveying of Acid-Tolerant Thermophilic Lignocellulolytic Fungi in Vietnam Reveals Surprisingly High Genetic Diversity. *Sci. Rep.* 9, 3674. doi:10.1038/s41598-019-40213-5
- Thompson, J. D., Higgins, D. G., and Gibson, T. J. (1994). CLUSTAL W: Improving the Sensitivity of Progressive Multiple Sequence Alignment through Sequence Weighting, Position-specific gap Penalties and Weight Matrix Choice. *Nucl. Acids Res.* 22, 4673–4680. doi:10.1093/nar/22.22.4673
- Tölgo, M., Hüttner, S., Rugbjerg, P., Thuy, N. T., Thanh, V. N., Larsbrink, J., et al. (2021). Genomic and Transcriptomic Analysis of the Thermophilic Lignocellulose-Degrading Fungus *Thielavia Terrestris* LPH172. *Biotechnol. Biofuels* 14, 131. doi:10.1186/s13068-021-01975-1
- UniProt Consortium (2019). UniProt: a Worldwide Hub of Protein Knowledge. *Nucleic Acids Res.* 47, D506–D515. doi:10.1093/nar/gky1049
- Vallim, M. A., Miller, K. Y., and Miller, B. L. (2000). *Aspergillus* SteA (Sterile12-like) Is a Homeodomain-C2/h2-Zn+2 finger Transcription Factor Required for Sexual Reproduction. *Mol. Microbiol.* 36, 290–301. doi:10.1046/j.1365-2958.2000.01874.x
- Vieira, A. A., Vianna, G. R., Carrijo, J., Aragão, F. J. L., and Vieira, P. M. (2021). Generation of *Trichoderma harzianum* with Pyr4 Auxotrophic Marker by Using the CRISPR/Cas9 System. *Sci. Rep.* 11 (1), 1085. doi:10.1038/s41598-020-80186-4
- Vieira, P. M., Zeilinger, S., Brandão, R. S., Vianna, G. R., Georg, R. C., Gruber, S., et al. (2018). Overexpression of an Aquaglyceroporin Gene in *Trichoderma harzianum* Affects Stress Tolerance, Pathogen Antagonism and Phaseolus vulgaris Development. *Biol. Control.* 126, 185–191. doi:10.1016/j.biocontrol.2018.08.012
- Whitehouse, D. G., May, B., and Moore, A. L. (2019). "Respiratory Chain and ATP Synthase," in *Reference Module in Biomedical Sciences* (Amsterdam: Elsevier). doi:10.1016/B978-0-12-801238-3.95732-5
- Wolfe, C. J., Kohane, I. S., and Butte, A. J. (2005). Systematic Survey Reveals General Applicability of "Guilt-By-Association" within Gene Coexpression Networks. *BMC Bioinformatics* 6, 227. doi:10.1186/1471-2105-6-227
- Wong Sak Hoi, J., and Dumas, B. (2010). Ste12 and Ste12-like Proteins, Fungal Transcription Factors Regulating Development and Pathogenicity. *Eukaryot. Cel* 9, 480–485. doi:10.1128/EC.00333-09
- Yan, L., and Khan, R. A. A. (2021). Biological Control of Bacterial Wilt in Tomato through the Metabolites Produced by the Biocontrol Fungus, *Trichoderma harzianum*. *Egypt. J. Biol. Pest Control.* 31, 5. doi:10.1186/s41938-020-00351-9
- Zeilinger, S., and Atanasova, L. (2020). "Sensing and Regulation of Mycoparasitism-Relevant Processes in *Trichoderma*," in *New and Future Developments in Microbial Biotechnology and Bioengineering*. Editors V. K. Gupta, S. Zeilinger, H. B. Singh, and I. Druzhinina (Amsterdam: Elsevier), 39–55. doi:10.1016/b978-0-12-819453-9.00002-7
- Zeilinger, S. (2004). Gene Disruption in *Trichoderma Atroviride* via Agrobacterium-mediated Transformation. *Curr. Genet.* 45 (1), 54–60. doi:10.1007/s00294-003-0454-8
- Zeilinger, S., Schmoll, M., Pail, M., Mach, R. L., and Kubicek, C. P. (2003). Nucleosome Transactions on the *Hypocrea Jecorina* (*Trichoderma Reesei*) Cellulase Promoter Cbh2 Associated with Cellulase Induction. *Mol. Gen. Genomics* 270, 46–55. doi:10.1007/s00438-003-0895-2
- Zhang, W., Kou, Y., Xu, J., Cao, Y., Zhao, G., Shao, J., et al. (2013). Two Major Facilitator Superfamily Sugar Transporters from *Trichoderma Reesei* and Their

- Roles in Induction of Cellulase Biosynthesis. *J. Biol. Chem.* 288, 32861–32872. doi:10.1074/jbc.M113.505826
- Zhang, Y., Yang, J., Luo, L., Wang, E., Wang, R., Liu, L., et al. (2020). Low-cost Cellulase-Hemicellulase Mixture Secreted by *Trichoderma harzianum* EM0925 with Complete Saccharification Efficacy of Lignocellulose. *Ijms* 21, 371. doi:10.3390/ijms21020371
- Zhang, Z.-Q., Wu, W.-W., Chen, J.-D., Zhang, G.-Y., Lin, J.-Y., Wu, Y.-K., et al. (2021). Weighted Gene Coexpression Network Analysis Reveals Essential Genes and Pathways in Bipolar Disorder. *Front. Psychiatry* 12. doi:10.3389/fpsyt.2021.553305

**Conflict of Interest:** The authors declare that the research was conducted in the absence of any commercial or financial relationships that could be construed as a potential conflict of interest.

**Publisher's Note:** All claims expressed in this article are solely those of the authors and do not necessarily represent those of their affiliated organizations, or those of the publisher, the editors and the reviewers. Any product that may be evaluated in this article, or claim that may be made by its manufacturer, is not guaranteed or endorsed by the publisher.

Copyright © 2022 Rosolen, Aono, Almeida, Ferreira Filho, Horta and De Souza. This is an open-access article distributed under the terms of the Creative Commons Attribution License (CC BY). The use, distribution or reproduction in other forums is permitted, provided the original author(s) and the copyright owner(s) are credited and that the original publication in this journal is cited, in accordance with accepted academic practice. No use, distribution or reproduction is permitted which does not comply with these terms.